ISSN 1949-8470 (online)

World Journal of *Radiology*

World J Radiol 2016 October 28; 8(10): 816-850

Published by Baishideng Publishing Group Inc

WJR World Journal of Radiology

A peer-reviewed, online, open-access journal of Radiology

Editorial Board

2014-2017

The *World Journal of Radiology* Editorial Board consists of 365 members, representing a team of worldwide experts in radiology. They are from 36 countries, including Afghanistan (1), Argentina (2), Australia (5), Austria (7), Belgium (2), Brazil (8), Canada (6), Chile (1), China (43), Croatia (1), Denmark (4), Egypt (6), France (5), Germany (22), Greece (10), India (12), Iran (6), Ireland (2), Israel (3), Italy (47), Japan (13), Netherlands (1), New Zealand (1), Pakistan (1), Poland (2), Portugal (1), Serbia (1), Singapore (3), Slovakia (1), South Korea (18), Spain (4), Sweden (2), Switzerland (4), Thailand (1), Turkey (26), United Kingdom (11), and United States (82).

Yue-Qi Zhu, *Shanghai*

Croatia

Goran Kusec, Osijek

Denmark

Poul E Andersen, *Odense*
Lars J Petersen, *Aalborg*
Thomas Z Ramsoy, *Frederiksberg*
Morten Ziebell, *Copenhagen*

Egypt

Mohamed F Bazeed, *Mansoura*
Mohamed Abou El-Ghar, *Mansoura*
Reem HA Mohamed, *Cairo*
Mohamed R Nouh, *Alexandria*
Ahmed AKA Razek, *Mansoura*
Ashraf A Zytoon, *Shebin El-Koom*

France

Sabine F Bensamoun, *Compiègne*
Romaric Loffroy, *Dijon*
Stephanie Nougaret, *Montpellier*
Hassane Oudadesse, *Rennes*
Vincent Vinh-Hung, *Fort-de-France*

Germany

Henryk Barthel, *Leipzig*
Peter Bannas, *Hamburg*
Martin Beeres, *Frankfurt*
Ilja F Ciernik, *Dessau*
A Dimitrakopoulou-Strauss, *Heidelberg*
Peter A Fasching, *Erlanegn*
Andreas G Schreyer, *Regensburg*
Philipp Heusch, *Duesseldorf*
Sonja M Kirchhoff, *Munich*
Sebastian Ley, *Munich*
Adel Maataoui, *Frankfurt am Main*
Stephan M Meckel, *Freiburg*
Hans W Muller, *Duesseldorf*
Kay Raum, *Berlin*
Dirk Rades, *Luebeck*
Marc-Ulrich Regier, *Hamburg*
Alexey Surov, *Halle*
Martin Walter, *Magdeburg*
Axel Wetter, *Essen*
Christoph Zilkens, *Düsseldorf*

Greece

Panagiotis Antoniou, *Thessaloniki*
Nikos Efthimiou, *Athens*
Dimitris Karnabatidis, *Patras*
George Latsios, *Athens*
Stylianos Megremis, *Iraklion*
Alexander D Rapidis, *Athens*
Kiki Theodorou, *Larissa*
Ioannis A Tsalafoutas, *Athens*
Evanthia E Tripoliti, *Ioannina*
Athina C Tsili, *Ioannina*

India

Ritesh Agarwal, *Chandigarh*
Chandan J Das, *New Delhi*
Prathamesh V Joshi, *Mumbai*
Naveen Kalra, *Chandigarh*
Chandrasekharan Kesavadas, *Trivandrum*
Jyoti Kumar, *New Delhi*
Atin Kumar, *New Delhi*
Kaushala P Mishra, *Allahabad*
Daya N Sharma, *New Delhi*
Binit Sureka, *New Delhi*
Sanjay Sharma, *New Delhi*
Raja R Yadav, *Allahabad*

Iran

Majid Assadi, *Bushehr*
SeyedReza Najafizadeh, *Tehran*
Mohammad Ali Oghabian, *Tehran*
Amir Reza Radmard, *Tehran*
Ramin Sadeghi, *Mashhad*
Hadi Rokni Yazdi, *Tehran*

Ireland

Tadhg Gleeson, *Wexford*
Frederik JAI Vernimmen, *Cork*

Israel

Dafna Ben Bashat, *Tel Aviv*
Amit Gefen, *Tel Aviv*
Tamar Sella, *Jerusalem*

Italy

Adriano Alippi, *Rome*
Dante Amelio, *Trento*
Michele Anzidei, *Rome*
Filippo F Angileri, *Messinas*
Stefano Arcangeli, *Rome*
Roberto Azzoni, *San Donato milanese*
Tommaso V Bartolotta, *Palermo*
Tommaso Bartalena, *Imola*
Livia Bernardin, *San Bonifacio*
Federico Boschi, *Verona*
Sergio Casciaro, *Lecce*
Emanuele Casciani, *Rome*
Musa M Can, *Napoli*
Alberto Cuocolo, *Napoli*
Michele Ferrara, *Coppito*
Mauro Feola, *Fossano*
Giampiero Francica, *Castel Volturno*
Luigi De Gennaro, *Rome*
Giulio Giovannetti, *Pisa*
Francesca Iacobellis, *Napoli*
Formato Invernizzi, *Monza Brianza*
Francesco Lassandro, *Naples*
Lorenzo Livi, *Florence*
Pier P Mainenti, *Napoli*
Laura Marzetti, *Chieti*
Giuseppe Malinverni, *Crescentino*
Enrica Milanesi, *Turin*
Giovanni Morana, *Treviso*
Lorenzo Monti, *Milan*
Silvia D Morbelli, *Genoa*
Barbara Palumbo, *Perugia*
Cecilia Parazzini, *Milan*
Stefano Pergolizzi, *Messina*
Antonio Pinto, *Naples*
Camillo Porcaro, *Rome*
Carlo C Quattrocchi, *Rome*
Alberto Rebonato, *Perugia*
Giuseppe Rizzo, *Rome*
Roberto De Rosa, *Naples*
Domenico Rubello, *Rovigo*
Andrea Salvati, *Bari*
Sergio Sartori, *Ferrara*
Luca M Sconfienza, *Milano*
Giovanni Storto, *Rionero*
Nicola Sverzellati, *Parma*
Alberto S Tagliafico, *Genova*
Nicola Troisi, *Florence*

Japan

Yasuhiko Hori, *Chiba*
Hidetoshi Ikeda, *Koriyama*
Masahito Kawabori, *Sapporo*
Tamotsu Kamishima, *Sapporo*
Hiro Kiyosue, *Yufu*
Yasunori Minami, *Osaka-sayama*
Yasuhiro Morimoto, *Kitakyushu*
Satoru Murata, *Tokyo*
Shigeki Nagamachi, *Miyazaki*
Hiroshi Onishi, *Yamanashi*
Morio Sato, *Wakayama Shi*
Yoshito Tsushima, *Maebashi*
Masahiro Yanagawa, *Suita*

Netherlands

Willem Jan van Rooij, *Tilburg*

New Zealand

W Howell Round, *Hamilton*

Pakistan

Wazir Muhammad, *Abbottabad*

Poland

Maciej S Baglaj, *Wroclaw*

Piotr Czauderna, *Gdansk*

Portugal

Joao Manuel RS Tavares, *Porto*

Serbia

Olivera Ciraj-Bjelac, *Belgrade*

Singapore

Gopinathan Anil, *Singapore*
Terence KB Teo, *Singapore*
Cher Heng Tan, *Singapore*

Slovakia

Stefan Sivak, *Martin*

South Korea

Ki Seok Choo, *Busan*
Seung Hong Choi, *Seoul*
Dae-Seob Choi, *Jinju*
Hong-Seok Jang, *Seoul*
Yong Jeong, *Daejeon*
Chan Kyo Kim, *Seoul*
Se Hyung Kim, *Seoul*
Joong-Seok Kim, *Seoul*
Sang Eun Kim, *Seongnam*
Sung Joon Kwon, *Seoul*
Jeong Min Lee, *Seoul*
In Sook Lee, *Busan*
Noh Park, *Goyang*
Chang Min Park, *Seoul*
Sung Bin Park, *Seoul*
Deuk Jae Sung, *Seoul*
Choongsoo Shin, *Seoul*
Kwon-Ha Yoon, *Iksan*

Spain

Miguel A De Gregorio, *Zaragoza*
Antonio Luna, *Jaén*
Enrique Marco de Lucas, *Santander*
Fernando Ruiz Santiago, *Granada*

Sweden

Dmitry Grishenkov, *Stockholm*
Tie-Qiang Li, *Stockholm*

Switzerland

Nicolau Beckmann, *Basel*
Christian Boy, *Bern*
Giorgio Treglia, *Bellinzona*

Stephan Ulmer, *Kiel*

Thailand

Sirianong Namwongprom, *Chiang Mai*

Turkey

Kubilay Aydin, *Istanbul*
Ramazan Akdemir, *Sakarya*
Serhat Avcu, *Ankara*
Ayse Aralasmak, *Istanbul*
Oktay Algin, *Ankara*
Nevbahar Akcar, *Meselik*
Bilal Battal, *Ankara*
Zulkif Bozgeyik, *Elazig*
Nazan Ciledag, Aakara
Fuldem Y Donmez, *Ankara*
Gulgun Engin, *Istanbul*
Ahmet Y Goktay, *Izmir*
Oguzhan G Gumustas, *Bursa*
Kaan Gunduz, *Ankara*
Pelin Ozcan Kara, *Mersin*
Kivanc Kamburoglu, *Ankara*
Ozgur Kilickesmez, *Istanbul*
Furuzan Numan, *Istanbul*
Cem Onal, *Adana*
Ozgur Oztekin, *Izmir*
Seda Ozbek (Boruban), *Konya*
Selda Sarikaya, *Zonguldak*
Figen Taser, *Kutahya*
Baran Tokar, *Eskisehir*
Ender Uysal, *Istanbul*
Ensar Yekeler, *Istanbul*

United Kingdom

Indran Davagnanam, *London*
M DC Valdés Hernández, *Edinburgh*
Alan Jackson, *Manchester*
Suneil Jain, *Belfast*
Long R Jiao, *London*
Miltiadis Krokidis, *Cambridge*
Pradesh Kumar, *Liverpool*
Peter D Kuzmich, *Derby*
Georgios Plataniotis, *Brighton*
Vanessa Sluming, *Liverpool*

United States

Garima Agrawal, *Saint Louis*
James R Brasic, *Baltimore*
Rajendra D Badgaiyan, *Buffalo*
Ulas Bagci, *Bethesda*
Anat Biegon, *Stony Brook*
Ramon Casanova, *Winston Salem*
Wenli Cai, *Boston*
Zheng Chang, *Durham*
Corey J Chakarun, *Long Beach*
Kai Chen, *Los Angeles*
Hyun-Soon Chong, *Chicago*
Marco Cura, *Dallas*
Ravi R Desai, *Bensalem*
Delia DeBuc, *Miami*
Carlo N De Cecco, *Charleston*
Timm-Michael L Dickfeld, *Baltimore*
Subba R Digumarthy, *Boston*
Huy M Do, *Stanford*
Todd A Faasse, *Grand Rapids*
Salomao Faintuch, *Boston*
Girish M Fatterpekar, *New York*
Dhakshinamoorthy Ganeshan, *Houston*
Robert J Griffin, *Little Rock*
Andrew J Gunn, *Boston*
Sandeep S Hedgire, *Boston*
Timothy J Hoffman, *Columbia*
Mai-Lan Ho, *San Francisco*
Juebin Huang, *Jackson*
Abid Irshad, *Charleston*
Matilde Inglese, *New York*
El-Sayed H Ibrahim, *Jacksonville*
Paul R Julsrud, *Rochester*
Pamela T Johnson, *Baltimore*
Ming-Hung Kao, *Tempe*
Sunil Krishnan, *Houston*
Richard A Komoroski, *Cincinnati*
Sandi A Kwee, *Honolulu*
King Kim, *Ft. Lauderdale*
Guozheng Liu, *Worcester*
Yiyan Liu, *Newark*
Venkatesh Mani, *New York*
Lian-Sheng Ma, *Pleasanton*
Rachna Madan, *Boston*
Zeyad A Metwalli, *Houston*
Yilong Ma, *Manhasset*
Hui Mao, *Atlanta*
Feroze B Mohamed, *Philadelphia*
Gul Moonis, *Boston*
John L Nosher, *New Brunswick*
Rahmi Oklu, *Boston*
Aytekin Oto, *Chicago*
Bishnuhari Paudyal, *Philadelphia*
Rajul Pandya, *Youngstown*
Chong-Xian Pan, *Sacramento*
Jay J Pillai, *Baltimore*
Neal Prakash, *Duarte*
Reza Rahbar, *Boston*
Ali S Raja, *Boston*
Gustavo J Rodriguez, *El Paso*
David J Sahn, *Portlsand*
Steven Schild, *Scottsdale*
Ali R Sepahdari, *Los Angeles*
Li Shen, *Indianapolis*
JP Sheehan, *Charlottesville*
Atul B Shinagare, *Boston*
Sarabjeet Singh, *Boston*
Charles J Smith, *Columbia*
Kenji Suzuki, *Chicago*
Monvadi Srichai-Parsia, *Washington*
Sree H Tirumani, *Boston*
Hebert A Vargas, *New York*
Sachit Verma, *Philadelphia*
Yoichi Watanabe, *Minneapolis*
Li Wang, *Chapel Hill*
Carol C Wu, *Boston*
Shoujun Xu, *Houston*
Min Yao, *Cleveland*
Xiaofeng Yang, *Atlanta*
Qingbao Yu, *Albuquerque*
Aifeng Zhang, *Chicago*
Chao Zhou, *Bethlehem*
Hongming Zhuang, *Philadelphia*

World Journal of Radiology

Contents

Monthly Volume 8 Number 10 October 28, 2016

World Journal of Radiology
Volume 8 Number 10 October 28, 2016

Contents

NAME OF JOURNAL
World Journal of Radiology

ISSN
ISSN 1949-8470 (online)

LAUNCH DATE
January 31, 2009

FREQUENCY
Monthly

EDITORIAL OFFICE
Xiu-Xia Song, Director
Fang-Fang Ji, Vice Director
World Journal of Radiology
Baishideng Publishing Group Inc
8226 Regency Drive, Pleasanton, CA 94588, USA
Telephone: +1-925-2238242
Fax: +1-925-2238243
E-mail: editorialoffice@wjgnet.com
Help Desk: http://www.wjgnet.com/esps/helpdesk.aspx
http://www.wjgnet.com

PUBLISHER
Baishideng Publishing Group Inc
8226 Regency Drive,
Pleasanton, CA 94588, USA
Telephone: +1-925-2238242
Fax: +1-925-2238243
E-mail: bpgoffice@wjgnet.com
Help Desk: http://www.wjgnet.com/esps/helpdesk.aspx
http://www.wjgnet.com

PUBLICATION DATE
October 28, 2016

INSTRUCTIONS TO AUTHORS
http://www.wjgnet.com/bpg/gerinfo/204

ONLINE SUBMISSION
http://www.wjgnet.com/esps/

World Journal of Radiology

Submit a Manuscript: http://www.wjgnet.com/esps/
Help Desk: http://www.wjgnet.com/esps/helpdesk.aspx
DOI: 10.4329/wjr.v8.i10.816

World J Radiol 2016 October 28; 8(10): 816-818
ISSN 1949-8470 (online)

FIELD OF VISION

Radium-223 and metastatic castration-resistant prostate cancer: All that glitters is not gold

Carlo Aprile, Marco G Persico, Lorenzo Lodola, Federica E Buroni

Carlo Aprile, Marco G Persico, Lorenzo Lodola, Federica E Buroni, Nuclear Medicine Unit, Department of Oncohaematology, Fondazione IRCCS Policlinico San Matteo, 27100 Pavia, Italy

Marco G Persico, Scuola Universitaria Superiore IUSS Pavia, 27100 Pavia, Italy

Author contributions: Aprile C wrote the manuscript; Aprile C, Persico MG, Lodola L and Buroni FE collected the material and discussed the topic.

Conflict-of-interest statement: Nothing to declare.

Manuscript source: Invited manuscript

Correspondence to: Carlo Aprile, MD, Nuclear Medicine Unit, Department of Oncohaematology, Fondazione IRCCS Policlinico San Matteo, v.le Golgi 19, 27100 Pavia, Italy. c.aprile@smatteo.pv.it
Telephone: +39-340-6415480
Fax: +39-038-2501669

Received: April 30, 2016
Peer-review started: May 3, 2016
First decision: July 6, 2016
Revised: August 4, 2016
Accepted: August 27, 2016
Article in press: August 29, 2016
Published online: October 28, 2016

Abstract

After being approved by the National Drug Agency in several countries, Radium-223 (Ra-223) is gaining wide acceptance in the treatment of bone metastatic castration resistant prostate cancer. The exact mechanism of action remain unclear: The established model of direct alpha-particle irradiation from the remodelling bone surface, where Ra-223 accumulates, surrounding the tumor foci can explain a lethal effect only on metastatic microdeposits, but not on higher tumor burden. According to the "pre-metastatic niche model", it is likely that Ra-223 targets several non-tumoral cell types of the tumor microenvironment involved in the complex mechanism of cancer bone homing and colonization. A deeper insight into this hypothetical mechanism will lead to a more accurate dosimetric approach and to find optimal sequencing and/or combination with the other therapeutic options.

Key words: Radium-223; Bone metastases; Castration resistant prostate cancer; Tumor microenvironment; Pre-metastatic niche model

Core tip: Radium-223, possible perspectives for a more effective use in bone metastatic castration resistant prostate cancer.

Aprile C, Persico MG, Lodola L, Buroni FE. Radium-223 and metastatic castration-resistant prostate cancer: All that glitters is not gold. *World J Radiol* 2016; 8(10): 816-818 Available from: URL: http://www.wjgnet.com/1949-8470/full/v8/i10/816.htm DOI: http://dx.doi.org/10.4329/wjr.v8.i10.816

COMMENTARY ON HOT TOPICS

Several therapeutic options have been shown to be clinically effective in treating metastatic castration resistant prostate cancer (mCRPC), albeit real efficacy of treatment is very difficult to establish due to a substantial

lack of head-to-head comparison trials. Radium-223 (Ra-223), an alpha-emitting radiopharmaceutical, prolongs overall survival (OS), delays symptomatic skeletal events and improves quality of life compared to placebo treatment, in patients with CRPC and symptomatic bone metastases without visceral involvement, regardless of prior docetaxel use[1,2].

The calcium mimetic alpha emitter ion Ra-223 forms complexes with hydroxyapatite in bone areas where turnover tissue is increased as in primary bone tumours and metastases. Unlike other therapeutic bone seekers, such as beta minus emitters Sr-89 or ^{153}Sm-EDTMP, Ra-223 has a high linear energy transfer (LET 80 keV/μm) leading to a high frequency of lethal double-strand DNA breaks in nearby cells[3].

The short path length of alpha particles is less than 100 μm, less than a 10 cell diameter and has an *in vitro* killing effect in tumor cells, osteoblasts and osteoclasts.

In vitro data demonstrates that the lethal effect is not cell type specific, is effective on multidrug resistant cells, induces G2 arrest and causes a dose-dependent inhibition of osteoclast differentiation[4-6].

The efficacy of Ra-223 has been demonstrated *in vivo* in animal models, indicating a significant antitumor effect in experimental skeletal metastases in nude rats[4], increased survival in a mouse model of breast cancer metastases, more pronounced if associated with zoledronic acid or doxorubicin[5].

These physical and biological data explain why Ra-223 is the first-in-class commercially available alpha emitter in the treatment of bone metastases. Results from a Phase Ⅲ trial called ALSYMPCA confirmed the clinical efficacy of the radiopharmaceutical in a large cohort of bone mCRPC[7]. However the mechanism of action remains unclear.

The most simplistic model that alpha emission acts directly on surrounding tumor cells is commonly accepted, even though its short path length can kill only a few tumor cells lines, much as the outer layers of an onion. Dosimetric considerations of this model indicate that the estimated absorbed dose in a 250 μm radius sphere decreases steeply from about 65 Gy at 5 μm from the surface to 0 Gy at 70 μm, assuming a Ra-223 concentration of 0.67 Bq/mm^2 on the surface[8]. In such a way, Ra-223 could deliver a lethal dose to small foci of cancer cells or micrometastases, while the dose to larger ones are likely to be ineffective.

Data from the ALSYMPCA trial indicate a significant decrease in PSA, regarding tumor burden and alkaline phosphatase (ALP) activity, the latter being a marker of bone turnover that correlates with the progression of bone metastases. The classical model cannot fully explain the therapeutic effect of Ra-223 in the presence of a large tumour burden in bone. Current treatment such as abiraterone targets cancer cells directly, while docetaxel acts indirectly on rapidly proliferating tissue. At present, only sipoleucel-T, whose mechanism of action involves the immune system, acts differently. Further questions remain to be answered as to why PCa displays an increased predilection for bone and why it induces an osteoblastic response. Just over a century ago, Paget proposed the "Seed and Soil" hypothesis. More recently, Lyden's laboratory[9] defined the "pre-metastatic niche model", where the remodelling of metastatic distant site occurs earlier than tumor cells detach from the primary site. Therefore the interaction between host and tumor or, in other words, the tumor microenvironment, may answer the above questions.

In a recent innovative paper Ganguly *et al*[10] reviewed the specific processes involved in the seeding and development of PCa bone metastases. Integrins, extracellular proteases and transient epithelial-mesenchymal transition can promote PCa progression, invasion and metastasis, just as chemotactic cytokines, adhesion molecules and bone derived signals can explain homing, colonization and osteoblastic characteristics. According to this model, many non-tumoral cell types could be the target of lethal alpha emission from Ra-223 leading to a "curative" effect, while the beta minus emission from Sr-89 and ^{153}Sm-EDTMP can obtain only a palliative effect.

Albeit preliminary, there is PET evidence indicating acute metabolic changes in large metastatic deposits after Ra-223 therapy, with a dramatic drop of uptake either of ^{18}F-choline[11] or ^{68}Ga-PSMA[12] in responders accompanied by a reduction of PSA and ALP. This effect cannot be explained by the classical mechanism of action where only a limited number of tumour cells can be hit, but rather by an effect on the microenvironment including vessels and stroma, inducing tumor regression.

The "niche model" could explain why the preventive administration of Ra-223 before cancer transplant in mice decreases the tumor burden and increases life expectancy[5]. In addition, Ra-223 uptake in the bone microenvironment surrounding metastatic foci is roughly the same in both osteolytic and osteoblastic tumours, opening new perspectives in the treatment of other cancer types[6].

Cancer cells with stem-cell like characteristics survive as non-proliferating (dormant) in close proximity to active bone multicellular units. They can survive after most therapeutic approaches including androgen deprivation and they start to proliferate receiving the appropriate signal from the stroma. Assuming that Ra-223 emissions act more likely and more efficiently on the microenvironment, they could have a role in the dormancy stage, inhibiting the metastatic growth.

It is quite surprising that basic research on Ra-223 was not oriented to study the effect of radiation to the cells involved in the niche model (homing, dormancy and proliferation) and the role of radiation to the vascular endothelium. In fact it is well known that Ra-223 accumulation did not correspond to bone volume or surface area but to local blood vessel density[6].

Median OS gain in the ALSYMPCA trial is 3.6 mo. Since 2010 six new agents have been approved for mCRPC, including chemotherapeutic agent, newer hormonal agents as enzalutamide and arabiterone, immune

therapy and bone-targeted agents as denosumab. However the Ra-223's OS gain is far to be optimal, as well as for the above mentioned agents. The main Health Technology Assessments, taking into account the cost per Quality Adjusted Life Years, concluded that Ra-223 therapy is not cost effective[13].

The integration of Ra-223 into the management of mCRPC with other currently available therapeutic options is likely to further improve OS[2,10]. This leads to further questions as to whether treatment should be started earlier in the course of mCRPC, a disease which frequently lasts several years, which is the best sequence of drugs or whether a combined therapy would be more effective than a sequential therapy[14].

The non-overlapping mechanism and the high safety profile of Ra-223 would potentially allow new combination strategies with the novel innovative drugs, moving from symptomatic high-volume bone disease to an earlier phase of asymptomatic low-volume bone disease and extending its use in the visceral disease phase if, as usually occurs, bone is involved[15].

These questions require a deeper insight into Ra-223's mechanism of action at the microenvironment level, thus allowing a more accurate dosimetric approach beyond activity/weight criteria.

ACKNOWLEDGMENTS

Authors wish to thank Professor Karen Susan Doyle for the language revision of the paper.

REFERENCES

1 **Nilsson S**. Radionuclide Therapies in Prostate Cancer: Integrating Radium-223 in the Treatment of Patients With Metastatic Castration-Resistant Prostate Cancer. *Curr Oncol Rep* 2016; **18**: 14 [PMID: 26779616 DOI: 10.1007/s11912-015-0495-4]

2 **Coleman R**. Treatment of Metastatic Bone Disease and the Emerging Role of Radium-223. *Semin Nucl Med* 2016; **46**: 99-104 [PMID: 26897713 DOI: 10.1053/j.semnuclmed.2015.10.012]

3 **Bruland ØS**, Nilsson S, Fisher DR, Larsen RH. High-linear energy transfer irradiation targeted to skeletal metastases by the alpha-emitter 223Ra: adjuvant or alternative to conventional modalities? *Clin Cancer Res* 2006; **12**: 6250s-6257s [PMID: 17062709 DOI: 10.1158/1078-0432.CCR-06-0841]

4 **Henriksen G**, Breistøl K, Bruland ØS, Fodstad Ø, Larsen RH. Significant antitumor effect from bone-seeking, alpha-particle-emitting (223)Ra demonstrated in an experimental skeletal metastases model. *Cancer Res* 2002; **62**: 3120-3125 [PMID: 12036923]

5 **Suominen MI**, Rissanen JP, Käkönen R, Fagerlund KM, Alhoniemi E, Mumberg D, Ziegelbauer K, Halleen JM, Käkönen SM, Scholz A. Survival benefit with radium-223 dichloride in a mouse model of breast cancer bone metastasis. *J Natl Cancer Inst* 2013; **105**: 908-916 [PMID: 23682134 DOI: 10.1093/jnci/djt116]

6 **Abou DS**, Ulmert D, Doucet M, Hobbs RF, Riddle RC, Thorek DL. Whole-Body and Microenvironmental Localization of Radium-223 in Naïve and Mouse Models of Prostate Cancer Metastasis. *J Natl Cancer Inst* 2016; **108**: pii: djv380 [PMID: 26683407 DOI: 10.1093/jnci/djv380]

7 **Parker C**, Nilsson S, Heinrich D, Helle SI, O'Sullivan JM, Fosså SD, Chodacki A, Wiechno P, Logue J, Seke M, Widmark A, Johannessen DC, Hoskin P, Bottomley D, James ND, Solberg A, Syndikus I, Kliment J, Wedel S, Boehmer S, Dall'Oglio M, Franzén L, Coleman R, Vogelzang NJ, O'Bryan-Tear CG, Staudacher K, Garcia-Vargas J, Shan M, Bruland ØS, Sartor O. Alpha emitter radium-223 and survival in metastatic prostate cancer. *N Engl J Med* 2013; **369**: 213-223 [PMID: 23863050 DOI: 10.1056/NEJMoa1213755]

8 **Henriksen G**, Fisher DR, Roeske JC, Bruland ØS, Larsen RH. Targeting of osseous sites with alpha-emitting 223Ra: comparison with the beta-emitter 89Sr in mice. *J Nucl Med* 2003; **44**: 252-259 [PMID: 12571218]

9 **Psaila B**, Lyden D. The metastatic niche: adapting the foreign soil. *Nat Rev Cancer* 2009; **9**: 285-293 [PMID: 19308068 DOI: 10.1038/nrc2621]

10 **Ganguly SS**, Li X, Miranti CK. The host microenvironment influences prostate cancer invasion, systemic spread, bone colonization, and osteoblastic metastasis. *Front Oncol* 2014; **4**: 364 [PMID: 25566502 DOI: 10.3389/fonc.2014.00364]

11 **Miyazaki KS**, Kuang Y, Kwee SA. Changes in Skeletal Tumor Activity on (18)F-choline PET/CT in Patients Receiving (223)Radium Radionuclide Therapy for Metastatic Prostate Cancer. *Nucl Med Mol Imaging* 2015; **49**: 160-164 [PMID: 26082811 DOI: 10.1007/s13139-014-0314-0]

12 **Ahmadzadehfar H**, Schlenkhoff CD, Rogenhofer S, Yordanova A, Essler M. 68Ga-PSMA-11 PET Represents the Tumoricidal Effect of 223Ra in a Patient With Castrate-Resistant Metastatic Prostate Cancer. *Clin Nucl Med* 2016; **41**: 695-696 [PMID: 27405025 DOI: 10.1097/RLU.0000000000001286]

13 **Norum J**, Traasdahl ER, Totth A, Nieder C, Olsen JA. Health Economics and Radium-223 (Xofigo®) in the Treatment of Metastatic Castration-Resistant Prostate Cancer (mCRPC): A Case History and a Systematic Review of the Literature. *Glob J Health Sci* 2016; **8**: 1-9 [PMID: 26573043 DOI: 10.5539/gjhs.v8n4p1]

14 **Park J**, Sartor AO, Sullivan R, King S, Antonarakis ES. Randomized phase-2 study of sipuleucel-T with or without radium-223 in men with asymptomatic/minimally symptomatic bone-metastatic castrate-resistant prostate cancer (CRPC). *J Clin Oncol* 2015; **33**: abstr TPS5076

15 **Lorente D**, Mateo J, Perez-Lopez R, de Bono JS, Attard G. Sequencing of agents in castration-resistant prostate cancer. *Lancet Oncol* 2015; **16**: e279-e292 [PMID: 26065613 DOI: 10.1016/S1470-2045(15)70033-1]

P- Reviewer: Kang TW, Vlachostergios PJ, Xia SJ **S- Editor**: Ji FF
L- Editor: A **E- Editor**: Li D

World Journal of Radiology

Submit a Manuscript: http://www.wjgnet.com/esps/
Help Desk: http://www.wjgnet.com/esps/helpdesk.aspx
DOI: 10.4329/wjr.v8.i10.819

World J Radiol 2016 October 28; 8(10): 819-828
ISSN 1949-8470 (online)

MINIREVIEWS

Blunt diaphragmatic lesions: Imaging findings and pitfalls

Matteo Bonatti, Fabio Lombardo, Norberto Vezzali, Giulia A Zamboni, Giampietro Bonatti

Matteo Bonatti, Norberto Vezzali, Giampietro Bonatti, Department of Radiology, Bolzano Central Hospital, 39100 Bolzano, Italy

Fabio Lombardo, Giulia A Zamboni, Department of Radiology, University of Verona, 37100 Verona, Italy

Author contributions: Bonatti M and Lombardo F wrote the paper; all the authors collaborated in data collection and paper review.

Conflict-of-interest statement: There is no conflict of interest associated with any of the senior author or other co-authors contributed their efforts in this manuscript.

Manuscript source: Invited manuscript

Correspondence to: Matteo Bonatti, MD, Department of Radiology, Bolzano Central Hospital, 5 Boehler St., 39100 Bolzano, Italy. matteobonatti@hotmail.com
Telephone: +39-0471-908494
Fax: +39-0471-908908

Received: March 30, 2016
Peer-review started: March 31, 2016
First decision: May 17, 2016
Revised: May 31, 2016
Accepted: August 27, 2016
Article in press: August 29, 2016
Published online: October 28, 2016

Abstract

Blunt diaphragmatic lesions (BDL) are uncommon in trauma patients, but they should be promptly recognized as a delayed diagnosis increases morbidity and mortality. It is well known that BDL are often overlooked at initial imaging, mainly because of distracting injuries to other organs. Sonography may directly depict BDL only in a minor number of cases. Chest X-ray has low sensitivity in detecting BDL and lesions can be reliably suspected only in case of intra-thoracic herniation of abdominal viscera. Thanks to its wide availability, time-effectiveness and spatial resolution, multi-detector computed tomography (CT) is the imaging modality of choice for diagnosing BDL; several direct and indirect CT signs are associated with BDL. Given its high tissue contrast resolution, magnetic resonance imaging can accurately depict BDL, but its use in an emergency setting is limited because of longer acquisition times and need for patient's collaboration.

Key words: Diaphragm; Blunt injury; Trauma; Imaging; Computed tomography

Core tip: Blunt diaphragmatic lesions (BDL) are uncommon, but they should be promptly recognized as a delayed diagnosis increases morbidity and mortality. We herein discuss multi-modality imaging findings in BDL and possible pitfalls in order to help the radiologist in this sometimes-difficult diagnosis.

Bonatti M, Lombardo F, Vezzali N, Zamboni GA, Bonatti G. Blunt diaphragmatic lesions: Imaging findings and pitfalls. *World J Radiol* 2016; 8(10): 819-828 Available from: URL: http://www.wjgnet.com/1949-8470/full/v8/i10/819.htm DOI: http://dx.doi.org/10.4329/wjr.v8.i10.819

INTRODUCTION

Blunt diaphragmatic lesions (BDL) represent a relatively

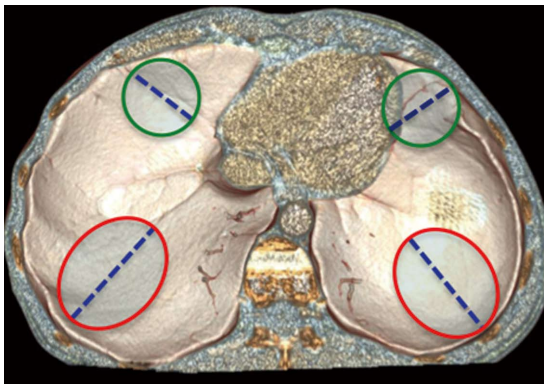

Figure 1 Physiological weakness points of the diaphragm. This volume-rendering reconstruction shows the most common sites of diaphragm rupture, which are located in the postero-lateral area (red circles) and in the antero-medial area (green circles) of each hemidiaphragm. Blunt diaphragmatic lesions usually show radial course (dotted lines).

uncommon event, with estimated prevalence of 0.2%-7% in patients admitted to an Emergency Department (ED) because of blunt trauma[1-3]. Although BDL are rarely life-threatening by themselves in the acute phase, patients suffering from BDL show high mortality rates, ranging from 5% to 50%, because of associated abdominal, thoracic and brain injuries[4-6]. Every diaphragmatic lesion should undergo surgical reparation as soon as possible in order to prevent further complications, like intestinal obstruction or respiratory distress, and to improve patient outcome[7]. Despite the need for an early diagnosis, BDL remain undiagnosed at initial imaging in 7%-66% of the cases[8-10], mainly because of the presence of distracting injuries. The aim of our work is to review imaging findings and possible pitfalls in patients with BDL in order to improve correct diagnosis rates.

Anatomical background and traumatic mechanisms

The diaphragm represents the anatomical landmark between thoracic and abdominal cavities and serves as the main muscle for respiration. Bilaterally, the diaphragm is composed by three main muscular groups, originating from the lumbar vertebrae, from the inferior border of the ribs and from the sternum, that converge into a thin strong central tendinous sheet. Bilaterally, in the sites where these muscular groups converge, the so-called lumbo-costal triangles and sterno-costal triangles, muscular fibers are replaced by thin areolar tissue, which constitutes a physiological weakness point. Moreover, the posterolateral area of each hemidiaphragm represents a weakness point also being the site where, during the 8th gestational week, the pleuroperitoneal membranes join with the septum trasversum to close the pleuroperitoneal hiatus.

BDL are usually the consequence of high-energy blunt abdominal traumas that determine a sudden increase in abdominal pressure[11], and motor-vehicle collisions represent the most common mechanism of injury. Abdominal pressure is transmitted to the diaphragm that may crack in its physiological weakness points. Less common traumatic mechanisms are represented by high-energy lateral impacts that cause chest wall distortion and subsequent diaphragm shearing, and by direct lacerations from fractured ribs.

In the majority of cases BDL show a radial course, starting from the postero-lateral areas of the diaphragm and extending towards the central ones (Figure 1) for at least 10 cm[12]. The breakage flaps usually remain close to each other during the early post-traumatic stages, but afterwards they tend to move away because of the difference between the positive intra-abdominal pressure and the negative pleural space one that causes intra-thoracic visceral herniation.

Left BDL are significantly more frequent than right ones (2:1-7:1 ratios), probably because of the protective effect of the liver on the right hemidiaphragm and of a relative weakness of the left hemidiaphragm itself. This difference might also be the consequence of a bias in patient selection: Indeed, right BDL remain undiagnosed at initial imaging with a significantly higher prevalence than left ones[13].

Clinical presentation, diagnosis and treatment

BDL are often asymptomatic in their acute phase, but rarely occur as isolated injuries, as other life-threatening lesions are associated in 50%-100% of cases. Splenic, hepatic and renal injuries are the most commonly associated abdominal lesions, whereas hemothorax, pneumothorax and rib fractures are the most frequent thoracic ones.

Intra-thoracic herniation of abdominal viscera represents a near-invariable consequence of BDL, which may manifest from few seconds to many months after trauma. Intra-thoracic viscera herniation also represents the premise for further complications like intestinal incarceration, strangulation and occlusion, but also respiratory insufficiency.

Being a clinical diagnosis of BDL virtually impossible, imaging plays a central role for this goal. However, it is well known that BDL often remains unrecognized at initial imaging, mainly because of the presence of distracting injuries, and may become manifest only later because of complications[5,14]. Delayed presentation is associated with increased morbidity and mortality[15,16].

Treatment of BDL implicates laparotomy in the majority of the cases, whereas laparoscopy and thoracotomy are less frequently performed[6]. Laparotomy is preferred in hemodynamically unstable patients and in patients with associated intra-abdominal injuries[11]. First of all the surgeon must carefully examine both hemidiaphragms and, in case of intra-thoracic viscera herniation, he must reposition the herniated viscera into the abdominal cavity. The diaphragmatic rupture can then be repaired by means of interrupted or continuous non-absorbable sutures and, finally, a chest tube should be placed in the affected pleural cavity. In case of large

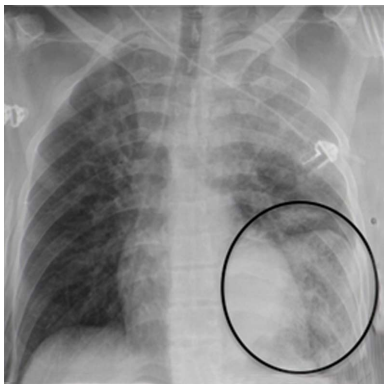

Figure 2 Chest X-ray findings in blunt diaphragmatic lesions. This antero-posterior chest X-ray shows viscera herniation in the thoracic cavity (circle) in association with costophrenic sulcus obliteration and distorted diaphragmatic profile.

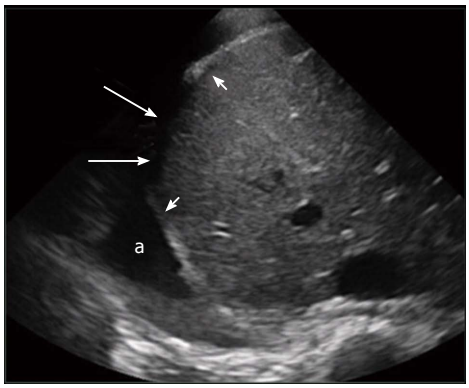

Figure 3 Sonographic findings in blunt diaphragmatic lesions. This transversal ultrasound scan directly shows the ruptured right hemidiaphragm (arrows) surrounded by thickened diaphragm edges (arrowheads). A good acoustic window is present due to a large pleural effusion (a).

diaphragmatic rupture a prosthetic patch can be used for closing the gap.

IMAGING OF BDL

Chest X-ray

Chest X-ray (CXR) is performed directly in the shock room in the majority of patients admitted to the ED because of blunt trauma[17]. Given the acute setting and the general conditions of the patients, CXR is usually performed by means of a single antero-posterior projection with the patient lying supine.

CXR has an unsatisfactory accuracy in detecting BDL; indeed, it may appear normal or it may show only nonspecific changes in 20%-50% of the patients affected by diaphragmatic rupture[18-21]. The only direct sign of BDL at chest radiogram is represented by the visualization of herniated bowel loops into the thoracic cavity (Figure 2). Bowel loops herniation may be appreciated directly or indirectly, because of nasogastric tube apex dislocation.

Some indirect signs might also be present, suggesting the possibility of BDL, but their sensitivity is extremely variable and their specificity is usually unsatisfactory. For example, hemidiaphragm elevation is strongly associated with BDL and previously published studies reported diagnostic accuracies of about 60%[9,22], but its specificity is extremely low, being often present in patients suffering from thoracic trauma. Other low-specificity signs associated with BDL are costophrenic sulcus obliteration and distorted diaphragmatic profile. In any case, the comparison with pre-trauma scans, whenever available, may increase the diagnostic performance by highlighting eventual post-traumatic changes.

Ultrasound

Sonography, usually in the form of fast scan, represents the first line imaging modality performed in the majority of blunt trauma patients admitted to the ED. At sonography the diaphragm can be recognized as a curved hyperechoic structure, with a homogeneous thickness, dividing the abdominal cavity from the thoracic one.

If a good thoracic acoustic window is present (*i.e.*, in case of large pleural effusions), in patients with large diaphragmatic ruptures ultrasound may directly depict the lesion as a focal interruption of the hyperechoic diaphragmatic line (Figure 3). Floating diaphragm edges and intra-thoracic visceral herniation may also be observed[23-25]. On the other hand, small diaphragmatic lesions can be hardly identified and the interpretation of diaphragmatic thickenings remains extremely debated.

Besides the direct visualization of the rupture, some indirect sonographic signs have also been associated with BDL. The impossibility of visualizing one or more hypochondriac organs or the heart without any particular technical factor able to explain it (the so-called "Rip's absent organ sign"[24]) in a patient admitted to the ED because of a severe blunt abdominal trauma, as well as the hypomobility of one hemidiaphragm in comparison to the other, should raise the suspicion of BDL. In these cases, further examinations, and in particular the performance of a contrast-enhanced multidetector computed tomography (MDCT) scan, are mandatory.

MDCT

MDCT has nowadays become the imaging modality of choice in trauma patients and also for diagnosing BDL. Indeed, thanks to the technological developments that lead to the introduction of multidetector scanners in the clinical practice, CT offers high accuracy (61%-87% sensitivity and 72%-100% specificity) in diagnosing BDL[26]. CT scans should be acquired with the patient lying supine on the table, with the hands over its head whenever possible; otherwise, the arms should be bent over a pillow on his abdomen in order to reduce beam hardening artifacts. The acquisition should be as fast as possible in order to prevent motion artifacts[27]. Contrast

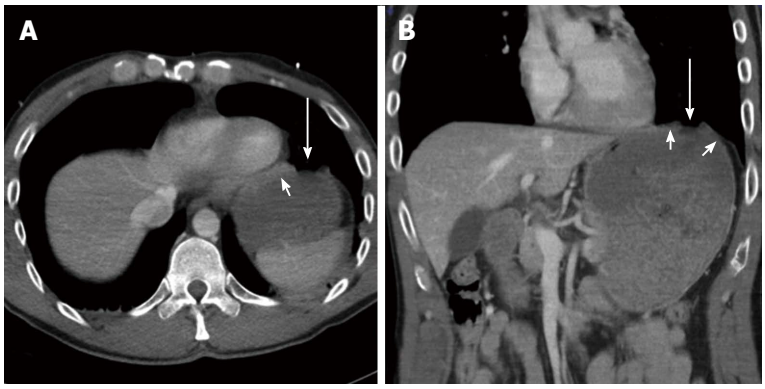

Figure 4 Computed tomography findings in blunt diaphragmatic lesions - segmental defect. These 3 mm thick axial (A) and coronal (B) multiplanar reconstructions show a segmental diaphragmatic defect (arrows) surrounded by diaphragmatic thickening that indicates muscle retraction (arrowheads).

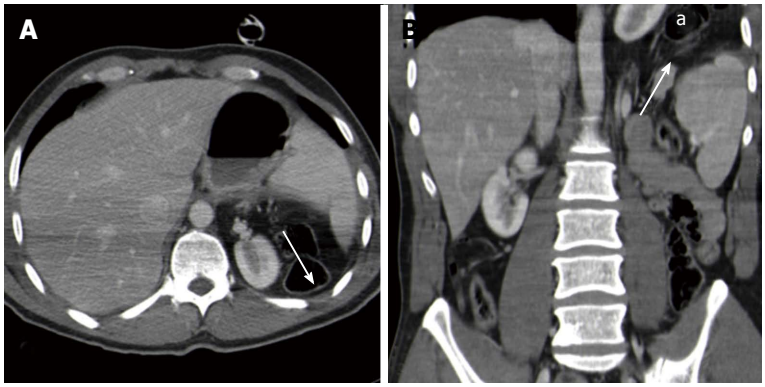

Figure 5 Computed tomography findings in blunt diaphragmatic lesions - diaphragm non-visualization. These 3 mm thick axial (A) and coronal (B) multiplanar reconstructions show a lack of diaphragm visualization, without the clear demonstration of a tear (arrows), associated with intra-thoracic viscera herniation (a).

material administration increases the conspicuity between different anatomical structures and, therefore, it is useful in order to better delimitate the diaphragm. Moreover, the evaluation of multiplanar reconstructions on sagittal and coronal planes increases CT accuracy in BDL detection[28,29].

CT often allows to directly depict diaphragmatic lesions as segmental defects; other direct signs of BDI are diaphragm non-visualization, dangling diaphragm sign and diaphragm thickening. Many different indirect signs have also been associated with BDL, *i.e.*, intra-thoracic viscera herniation, dependent viscera sign, collar sign and hump and band sign.

A segmental diaphragmatic defect (Figure 4) represents the most commonly encountered sign of BDL, with sensitivity values up to 95.7% in the most recent Literature[26,30]. The defect can be better appreciated on multiplanar reconstructions performed perpendicular to the tear than on axial images[31]. In the majority of the cases, the defect is delimited by slightly thickened diaphragmatic edges, as a consequence of edema, intramuscular hematoma and muscle retraction. Attention must be paid to physiological diaphragmatic defects, which may be observed in up to 11% of healthy population, with a prevalence that increases with age[32]: In these cases, no edge thickening is observed. In case of large diaphragmatic lesions, partial or complete diaphragm non-visualization (Figure 5) represents a relatively frequent event and it is almost always associated with intra-thoracic viscera herniation. The retracted diaphragm may be sometimes recognized at its bone insertion. The sensitivity of this sign is not as high as that of a simple diaphragmatic defect, but its specificity approaches 100%. Intra-thoracic viscera herniation (Figure 6) represents the direct consequence of the difference between intra-abdominal and intra-thoracic pressure, which brings the abdominal organs to herniate in the thoracic cavity if a large-enough diaphragmatic lesion is present. Viscera herniation is more common on the left than on the right side, because of the lack of the protective effect of the liver. Herniation probability increases parallel to tear extension. Intrapericardial herniation represents a rare but potentially fatal event[19].

Diaphragm thickening (Figure 7) is usually present in association with other signs of diaphragm rupture, but it may also be the only finding of small BDL. In high-energy blunt traumas, diaphragm thickness should be always accurately compared with the contralateral side in order to rule out a lesion. Diaphragm thickening may be the consequence of muscular edema or

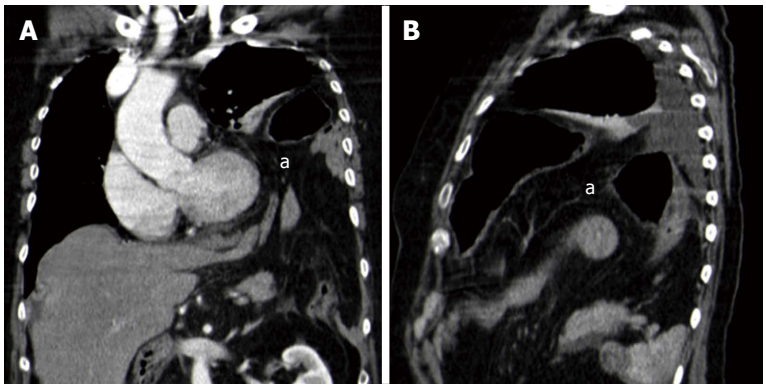

Figure 6 Computed tomography findings in blunt diaphragmatic lesions - intrathoracic viscera herniation. These 3 mm thick coronal (A) and sagittal (B) multiplanar reconstructions show intrathoracic herniation of abdominal organs and fat (a). This finding is often associated with diaphragm non-visualization or with large diaphragmatic defects.

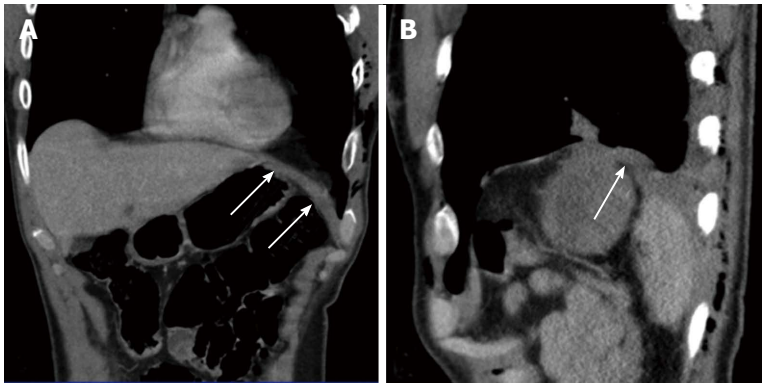

Figure 7 Computed tomography findings in blunt diaphragmatic lesions - diaphragm thickening. These 3 mm thick coronal (A) and sagittal (B) multiplanar reconstructions show an abnormally thickened left hemidiaphragm (arrows), highly suspicious for blunt diaphragmatic lesions in a patients with multiple ribs fractures and pneumothorax.

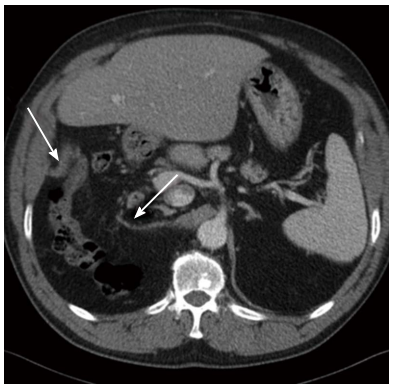

Figure 8 Computed tomography findings in blunt diaphragmatic lesions - dangling diaphragm sign. This 3 mm thick multiplanar axial reconstruction shows the free edges of a torn diaphragm as "comma-shaped" structures (arrows) which curl inward, toward the center of the abdomen. This alteration represents the so-called "dangling diaphragm sign".

hematoma, but it may also be the indicator of a still-closed diaphragmatic tear; therefore, this finding should be always highlighted in the radiological report and, in case of patients without any other indication for surgical exploration, it must be strictly followed-up by means of CT. Anyway, some variability in diaphragmatic thickness may be physiological[12].

The dangling diaphragm sign (Figure 8) was first described by Desser *et al*[33] in 2010 as the visualization of the free edges of the torn diaphragm as comma-shaped structures, which curl inward, toward the center of the abdomen. It is usually associated with a segmental diaphragmatic defect and diaphragm thickening. The dangling diaphragm sign may be observed in only about 50% of the patients with BDL, but its specificity reaches 98%[26,30,33].

The dependent viscera sign[34] (Figure 9) (also referred to as sinus cutoff sign[35]) was first described by Bergin *et al*[34] in 2001 and is represented by an anomalous contact between abdominal viscera and posterior chest wall, without the physiological lung parenchyma interposition. It is the consequence of the loss of the diaphragmatic support to the abdominal organs that, therefore, in the supine position tend to lie dorsally. It was particularly useful for BDL detection in the pre-multiplanar reconstructions era.

The collar sign (also referred to as hourglass sign) (Figure 10) is represented by a "waist-like" constriction

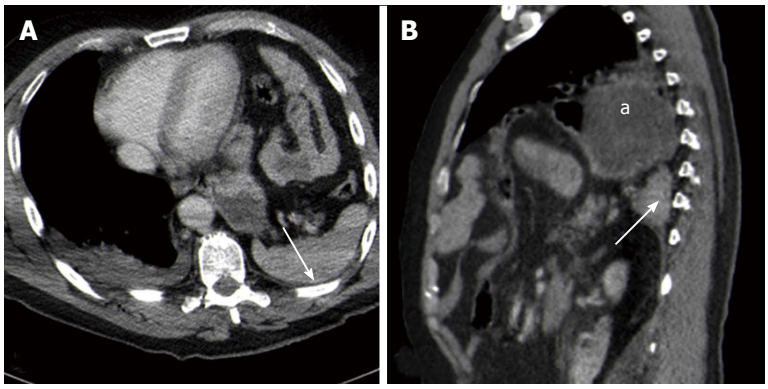

Figure 9 Computed tomography findings in blunt diaphragmatic lesions - dependent viscera sign. These 3 mm thick multiplanar axial (A) and coronal (B) reconstructions show the spleen (arrows) and the stomach (a) lying on the posterior chest wall, without lung parenchyma interposition. This alteration represents the so-called "dependent viscera sign".

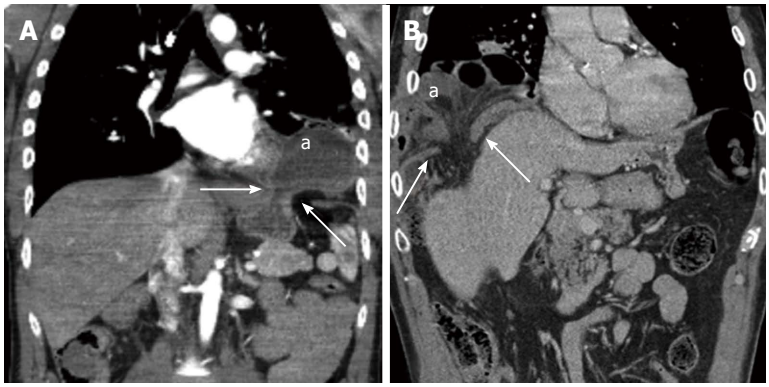

Figure 10 Computed tomography findings in blunt diaphragmatic lesions - collar sign. These 3 mm thick multiplanar coronal reconstructions (2 different patients, A and B) show intrathoracic herniation of the stomach (A, "a") and of the right colic flexure (B, "a"). In both cases the herniated material shows a hourglass shape as a consequence of the compression exerted on it by the ruptured diaphragm edges (arrows).

of the herniated viscera at the point of diaphragmatic discontinuity and is typically observed in case of left diaphragmatic lesions with gastric herniation. The hump and band sign (Figure 11) is similar to the collar sign and refers to the shape of the herniated liver in case of right BDL. The hump shape is due to the squeezing of the herniated liver above the diaphragmatic defect, whereas the hypoattenuating band is thought to be the consequence of local liver parenchyma hypoperfusion because of diaphragmatic compression. It is best appreciated on sagittal and coronal reconstructions.

The radiologist must pay particular attention to the above-mentioned signs in patients with parenchymal organs lesions, rib fractures, pleural effusion, hemothorax or hemoperitoneum.

Magnetic resonance imaging

Magnetic resonance imaging (MRI) warrants higher tissue contrast resolution than CT and enables to clearly depict the diaphragm (Figure 12), but its use in an emergency setting is limited by the longer acquisition times and by the need for patient collaboration. Moreover, the original advantage of MRI in comparison with CT in diagnosing BDL, *i.e.*, its multiplanarity, has been overwhelmed by the development of multidetector CT scanners. Therefore, nowadays MRI should be considered a second level investigation reserved to hemodynamically stable patients with inconclusive findings at CT[36].

In order to better evaluate the hemidiaphragms, MRI sequences should be acquired using cardiac and respiratory gating. The examination can be simply based on spin-echo T1-weighted sequences, acquired on the axial, sagittal and coronal planes, in which the normal diaphragm appears as a continuous hypointense band surrounded by hyperintense abdominal and subpleural fat[37]. In this setting, diaphragmatic discontinuities as well as the other findings described for CT may be accurately recognized[38,39]. Gradient-echo T1-weighted sequences represent an alternative to SE ones because of faster acquisition times, but chemical shift artifacts may limit their value.

PITFALLS IN BDL EVALUATION

False negative cases

Slight alterations, like slight diaphragmatic thickenings (Figure 13) or small diaphragmatic defects, may often remain undiagnosed at initial imaging, especially if major

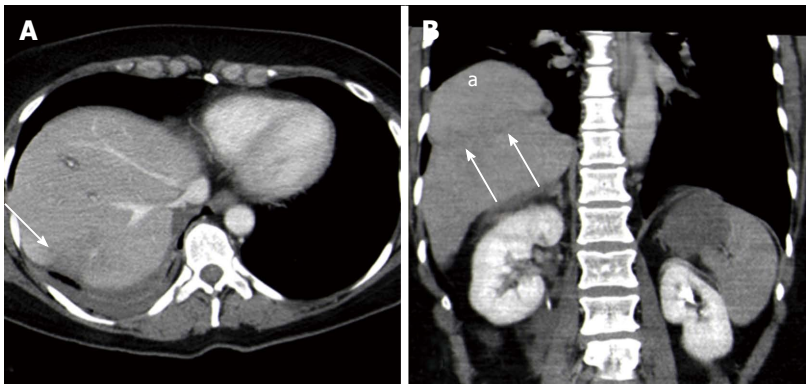

Figure 11 Computed tomography findings in blunt diaphragmatic lesions - hump and band sign. These 3 mm thick multiplanar axial (A) and coronal (B) reconstructions show a hypodense band that crosses the liver parenchyma in the site where it crosses the ruptured diaphragm (arrows), whereas the liver dome expands above it. This alteration represents the so-called "hump and band sign" (a).

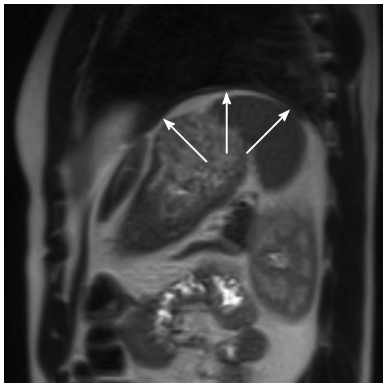

Figure 12 Magnetic resonance imaging apperarance of the diaphragm. This TSE T2-weighted sagittal image shows the left hemidiaphragm as an uniformly thin intermediate signal intensity band (arrows) between lung parenchyma and intra-abdominal fat.

distracting injuries are present, and may manifest only later because of complications. In the matter of facts, the presence of severe thoraco-abdominal injuries should point the radiologist's attention to the diaphragm.

BDL diagnosis may be more difficult in patients receiving mechanical ventilation, in particular if positive pressures are adopted[40]. Indeed, mechanical ventilation reduces the difference between intra-abdominal and intra-thoracic pressure, preventing abdominal viscera herniation (Figure 14) and reducing lesion conspicuity.

False positive cases

Eventration (Figure 15) may involve an entire hemi-diaphragm or only a part of it. In both cases muscle continuity must be clearly recognizable and no abnormal diaphragmatic thickenings must be observed; on the other hand, in case of eventration the involved diaphragm is usually uniformly thinned.

Congenital hernias (Figure 16) are usually located in the same areas where traumatic lesions occur and, therefore, the differential diagnosis may be particularly challenging. However, congenital hernias are usually not associated with diaphragm thickening.

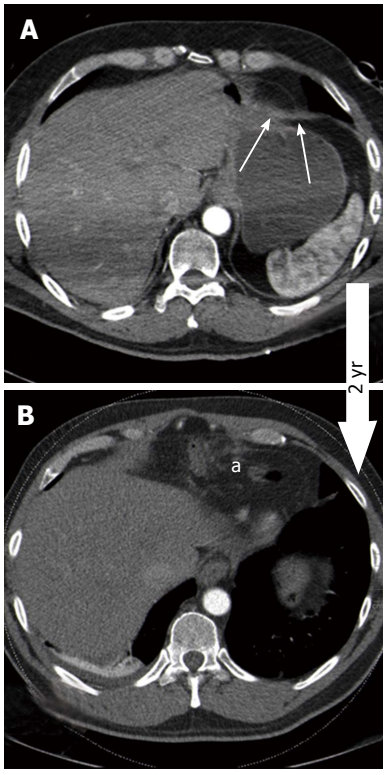

Figure 13 False negative case of blunt diaphragmatic lesions. Three millimeters thick axial CT images of the same patient, acquired after a precipitation trauma (A) and two years later (B). Thickening of the antero-medial part of the left hemidiaphragm (A, arrows) was overlooked at the first CT scan, performed after a precipitation trauma. Two years later, a CT scan performed because of epigastric pain showed intra-thoracic viscera herniation (B, "a") as a consequence of diaphragmatic rupture. CT: Computed tomography.

CONCLUSION

In the era of multidetector CT and of high quality multiplanar reconstructions, the diagnosis of BDL should be no more overlooked by radiologists working in an emergency setting. Appropriate knowledge of the common and less common signs of BDL and careful evaluation of the diaphragm in patients with blunt trauma should enable a timely and accurate diagnosis.

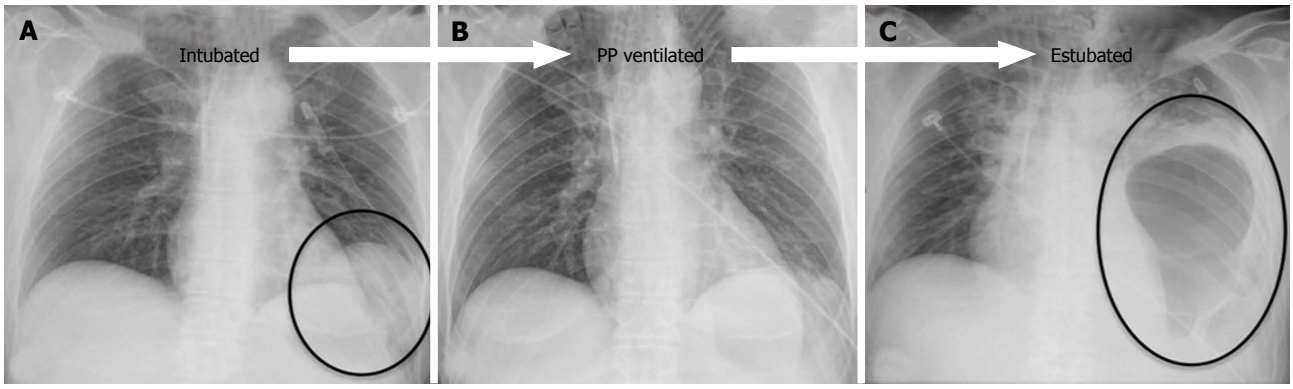

Figure 14 Effects of mechanical ventilation on blunt diaphragmatic lesions. The antero-posterior chest X-ray, performed immediately after intubation and left pneumothorax drainage (A) in a patient admitted to the ED because of severe motorbike accident, showed a double left diaphragmatic profile (circle), suspicious for BDI. The finding was not confirmed at the subsequent CT, performed after the beginning of positive-pressure ventilation, and also the CXR performed 2 d later, after pleural drainage removal (B) did not show any diaphragm alteration. Three days later, after estubation, the patient suffered respiratory insufficiency and left pleural drainage was replaced in the suspicion of relapsing pneumothorax; subsequent CXR (C) clearly demonstrated the presence of BDI with intra-thoracic gastric herniation (circle). BDI: Blunt diaphragmatic lesions; CXR: Chest X-ray; CT: Computed tomography; ED: Emergency Department.

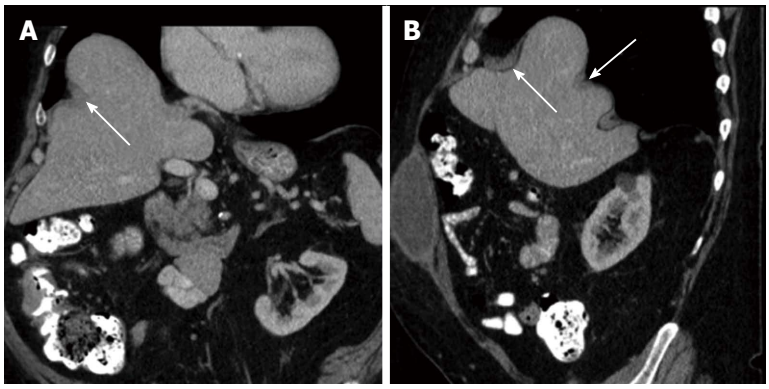

Figure 15 Diaphragm eventration. A and B: Eventration may mimick blunt diaphragmatic lesions. In case of eventration diaphragm continuity (arrows) must always be recongnizable and no abrupt thickness changes should be observed.

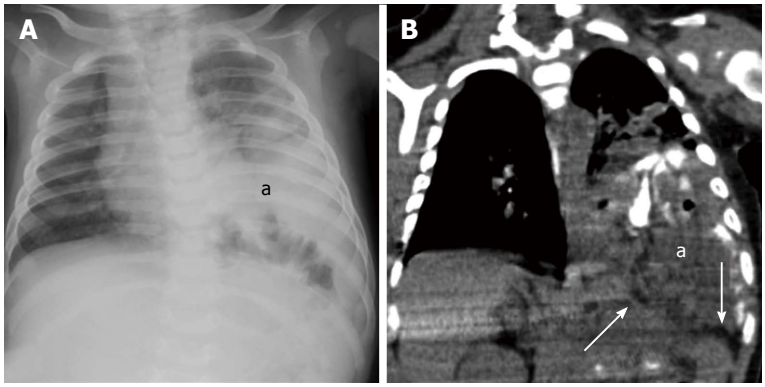

Figure 16 Congenital diaphragmatic hernia. CXR (A) and CT scan (B) of a 3-mo-old patient with congenital left diaphragmatic hernia (a). The diaphragmatic edges are not thickened (arrows). CXR: Chest X-ray; CT: Computed tomography.

REFERENCES

1 **Rodriguez-Morales G**, Rodriguez A, Shatney CH. Acute rupture of the diaphragm in blunt trauma: analysis of 60 patients. *J Trauma* 1986; **26**: 438-444 [PMID: 3701892 DOI: 10.1097/00005373-198605000-00005]

2 **Sliker CW**. Imaging of diaphragm injuries. *Radiol Clin North Am* 2006; **44**: 199-211, vii [PMID: 16500203 DOI: 10.1016/j.rcl.2005.10.003]

3 **Hsee L**, Wigg L, Civil I. Diagnosis of blunt traumatic ruptured diaphragm: is it still a difficult problem? *ANZ J Surg* 2010; **80**: 166-168 [PMID: 20575919 DOI: 10.1111/j.1445-2197.2009.05042.x]

4 **Haciibrahimoglu G**, Solak O, Olcmen A, Bedirhan MA, Solmazer N, Gurses A. Management of traumatic diaphragmatic rupture. *Surg Today* 2004; **34**: 111-114 [PMID: 14745609 DOI: 10.1007/s00595-003-2662-8]

5 **Mihos P**, Potaris K, Gakidis J, Paraskevopoulos J, Varvatsoulis P, Gougoutas B, Papadakis G, Lapidakis E. Traumatic rupture of the diaphragm: experience with 65 patients. *Injury* 2003; **34**: 169-172 [PMID: 12623245 DOI: 10.1016/S0020-1383(02)00369-8]

6 **Chughtai T**, Ali S, Sharkey P, Lins M, Rizoli S. Update on managing diaphragmatic rupture in blunt trauma: a review of 208 consecutive cases. *Can J Surg* 2009; **52**: 177-181 [PMID: 19503660]

7 **Iochum S**, Ludig T, Walter F, Sebbag H, Grosdidier G, Blum AG. Imaging of diaphragmatic injury: a diagnostic challenge? *Radiographics* 2002; **22** Spec No: S103-S116; discussion S116-S118 [PMID: 12376604 DOI: 10.1148/radiographics.22.suppl_1.g02oc14s103]

8 **Desir A**, Ghaye B. CT of blunt diaphragmatic rupture. *Radiographics* 2012; **32**: 477-498 [PMID: 22411944 DOI: 10.1148/rg.322115082]

9 **Guth AA**, Pachter HL, Kim U. Pitfalls in the diagnosis of blunt diaphragmatic injury. *Am J Surg* 1995; **170**: 5-9 [PMID: 7793494 DOI: 10.1016/S0002-9610(99)80242-6]

10 **Murray JG**, Caoili E, Gruden JF, Evans SJ, Halvorsen RA, Mackersie RC. Acute rupture of the diaphragm due to blunt trauma: diagnostic sensitivity and specificity of CT. *AJR Am J Roentgenol* 1996; **166**: 1035-1039 [PMID: 8615237 DOI: 10.2214/ajr.166.5.8615237]

11 **Tan KK**, Yan ZY, Vijayan A, Chiu MT. Management of diaphragmatic rupture from blunt trauma. *Singapore Med J* 2009; **50**: 1150-1153 [PMID: 20087550]

12 **Bocchini G**, Guida F, Sica G, Codella U, Scaglione M. Diaphragmatic injuries after blunt trauma: are they still a challenge? Reviewing CT findings and integrated imaging. *Emerg Radiol* 2012; **19**: 225-235 [PMID: 22362421 DOI: 10.1007/s10140-012-1025-4]

13 **Walchalk LR**, Stanfield SC. Delayed presentation of traumatic diaphragmatic rupture. *J Emerg Med* 2010; **39**: 21-24 [PMID: 18486412 DOI: 10.1016/j.jemermed.2007.09.044]

14 **Kuo IM**, Liao CH, Hsin MC, Kang SC, Wang SY, Ooyang CH, Fang JF. Blunt diaphragmatic rupture--a rare but challenging entity in thoracoabdominal trauma. *Am J Emerg Med* 2012; **30**: 919-924 [PMID: 21641158 DOI: 10.1016/j.ajem.2011.03.014]

15 **Ganie FA**, Lone H, Lone GN, Wani ML, Ganie SA, Wani NU, Gani M. Delayed presentation of traumatic diaphragmatic hernia: a diagnosis of suspicion with increased morbidity and mortality. *Trauma Mon* 2013; **18**: 12-16 [PMID: 24350143 DOI: 10.5812/traumamon.7125]

16 **Brasel KJ**, Borgstrom DC, Meyer P, Weigelt JA. Predictors of outcome in blunt diaphragm rupture. *J Trauma* 1996; **41**: 484-487 [PMID: 8810967 DOI: 10.1097/00005373-199609000-00016]

17 **Aukema TS**, Beenen LF, Hietbrink F, Leenen LP. Initial assessment of chest X-ray in thoracic trauma patients: Awareness of specific injuries. *World J Radiol* 2012; **4**: 48-52 [PMID: 22423318 DOI: 10.4329/wjr.v4.i2.48]

18 **Shackleton KL**, Stewart ET, Taylor AJ. Traumatic diaphragmatic injuries: spectrum of radiographic findings. *Radiographics* 1998; **18**: 49-59 [PMID: 9460108 DOI: 10.1148/radiographics.18.1.9460108]

19 **Mirvis SE**, Shanmuganagthan K. Imaging hemidiaphragmatic injury. *Eur Radiol* 2007; **17**: 1411-1421 [PMID: 17308925 DOI: 10.1007/s00330-006-0553-2]

20 **Sangster G**, Ventura VP, Carbo A, Gates T, Garayburu J, D'Agostino H. Diaphragmatic rupture: a frequently missed injury in blunt thoracoabdominal trauma patients. *Emerg Radiol* 2007; **13**: 225-230 [PMID: 17136377 DOI: 10.1007/s10140-006-0548-y]

21 **Langdorf MI**, Medak AJ, Hendey GW, Nishijima DK, Mower WR, Raja AS, Baumann BM, Anglin DR, Anderson CL, Lotfipour S, Reed KE, Zuabi N, Khan NA, Bithell CA, Rowther AA, Villar J, Rodriguez RM. Prevalence and Clinical Import of Thoracic Injury Identified by Chest Computed Tomography but Not Chest Radiography in Blunt Trauma: Multicenter Prospective Cohort Study. *Ann Emerg Med* 2015; **66**: 589-600 [PMID: 26169926 DOI: 10.1016/j.annemergmed.2015.06.003]

22 **Gelman R**, Mirvis SE, Gens D. Diaphragmatic rupture due to blunt trauma: sensitivity of plain chest radiographs. *AJR Am J Roentgenol* 1991; **156**: 51-57 [PMID: 1898570 DOI: 10.2214/ajr.156.1.1898570]

23 **Blaivas M**, Brannam L, Hawkins M, Lyon M, Sriram K. Bedside emergency ultrasonographic diagnosis of diaphragmatic rupture in blunt abdominal trauma. *Am J Emerg Med* 2004; **22**: 601-604 [PMID: 15666270 DOI: 10.1016/j.ajem.2004.08.015]

24 **Gangahar R**, Doshi D. FAST scan in the diagnosis of acute diaphragmatic rupture. *Am J Emerg Med* 2010; **28**: 387.e1-387.e3 [PMID: 20223407 DOI: 10.1016/j.ajem.2009.07.004]

25 **Kim HH**, Shin YR, Kim KJ, Hwang SS, Ha HK, Byun JY, Choi KH, Shinn KS. Blunt traumatic rupture of the diaphragm: sonographic diagnosis. *J Ultrasound Med* 1997; **16**: 593-598 [PMID: 9321778]

26 **Panda A**, Kumar A, Gamanagatti S, Patil A, Kumar S, Gupta A. Traumatic diaphragmatic injury: a review of CT signs and the difference between blunt and penetrating injury. *Diagn Interv Radiol* 2014; **20**: 121-128 [PMID: 24412818 DOI: 10.5152/dir.2013.13248]

27 **Liang T**, McLaughlin P, Arepalli CD, Louis LJ, Bilawich AM, Mayo J, Nicolaou S. Dual-source CT in blunt trauma patients: elimination of diaphragmatic motion using high-pitch spiral technique. *Emerg Radiol* 2016; **23**: 127-132 [PMID: 26637401 DOI: 10.1007/s10140-015-1365-y]

28 **Bhullar IS**, Block EF. CT with coronal reconstruction identifies previously missed smaller diaphragmatic injuries after blunt trauma. *Am Surg* 2011; **77**: 55-58 [PMID: 21396306]

29 **Larici AR**, Gotway MB, Litt HI, Reddy GP, Webb WR, Gotway CA, Dawn SK, Marder SR, Storto ML. Helical CT with sagittal and coronal reconstructions: accuracy for detection of diaphragmatic injury. *AJR Am J Roentgenol* 2002; **179**: 451-457 [PMID: 12130450 DOI: 10.2214/ajr.179.2.1790451]

30 **Hammer MM**, Flagg E, Mellnick VM, Cummings KW, Bhalla S, Raptis CA. Computed tomography of blunt and penetrating diaphragmatic injury: sensitivity and inter-observer agreement of CT Signs. *Emerg Radiol* 2014; **21**: 143-149 [PMID: 24142265 DOI: 10.1007/s10140-013-1166-0]

31 **Killeen KL**, Mirvis SE, Shanmuganathan K. Helical CT of diaphragmatic rupture caused by blunt trauma. *AJR Am J Roentgenol* 1999; **173**: 1611-1616 [PMID: 10584809 DOI: 10.2214/ajr.173.6.10584809]

32 **Caskey CI**, Zerhouni EA, Fishman EK, Rahmouni AD. Aging of the diaphragm: a CT study. *Radiology* 1989; **171**: 385-389 [PMID: 2704802 DOI: 10.1148/radiology.171.2.2704802]

33 **Desser TS**, Edwards B, Hunt S, Rosenberg J, Purtill MA, Jeffrey RB. The dangling diaphragm sign: sensitivity and comparison with existing CT signs of blunt traumatic diaphragmatic rupture. *Emerg Radiol* 2010; **17**: 37-44 [PMID: 19449046 DOI: 10.1007/s10140-009-0819-5]

34 **Bergin D**, Ennis R, Keogh C, Fenlon HM, Murray JG. The "dependent viscera" sign in CT diagnosis of blunt traumatic diaphragmatic rupture. *AJR Am J Roentgenol* 2001; **177**: 1137-1140 [PMID: 11641188 DOI: 10.2214/ajr.177.5.1771137]

35 **Kaya SO**, Karabulut N, Yuncu G, Sevinc S, Kiroğlu Y. Sinus cut-off sign: a helpful sign in the CT diagnosis of diaphragmatic rupture associated with pleural effusion. *Eur J Radiol* 2006; **59**: 253-256 [PMID: 16762521 DOI: 10.1016/j.ejrad.2006.04.015]

36 **Eren S**, Kantarci M, Okur A. Imaging of diaphragmatic rupture after trauma. *Clin Radiol* 2006; **61**: 467-477 [PMID: 16713417 DOI: 10.1016/j.crad.2006.02.006]

37 **Gierada DS**, Curtin JJ, Erickson SJ, Prost RW, Strandt JA, Goodman LR. Diaphragmatic motion: fast gradient-recalled-echo MR imaging in healthy subjects. *Radiology* 1995; **194**: 879-884 [PMID: 7862995 DOI: 10.1148/radiology.194.3.7862995]

38 **Barbiera F**, Nicastro N, Finazzo M, Lo Casto A, Runza G, Bartolotta TV, Midiri M. The role of MRI in traumatic rupture of the diaphragm. Our experience in three cases and review of the literature. *Radiol Med* 2003; **105**: 188-194 [PMID: 12835642]

39 **Shanmuganathan K**, Mirvis SE, White CS, Pomerantz SM. MR

imaging evaluation of hemidiaphragms in acute blunt trauma: experience with 16 patients. *AJR Am J Roentgenol* 1996; **167**: 397-402 [PMID: 8686615 DOI: 10.2214/ajr.167.2.8686615]

40 **Karmy-Jones R**, Carter Y, Stern E. The impact of positive pressure ventilation on the diagnosis of traumatic diaphragmatic injury. *Am Surg* 2002; **68**: 167-172 [PMID: 11842965]

P- Reviewer: Lovric Z, Slomiany BL **S- Editor**: Ji FF **L- Editor**: A
E- Editor: Li D

World Journal of Radiology

Submit a Manuscript: http://www.wjgnet.com/esps/
Help Desk: http://www.wjgnet.com/esps/helpdesk.aspx
DOI: 10.4329/wjr.v8.i10.829

World J Radiol 2016 October 28; 8(10): 829-845
ISSN 1949-8470 (online)

SYSTEMATIC REVIEWS

Role of molecular imaging in the management of patients affected by inflammatory bowel disease: State-of-the-art

Federico Caobelli, Laura Evangelista, Natale Quartuccio, Demetrio Familiari, Corinna Altini, Angelo Castello, Mariapaola Cucinotta, Rossella Di Dato, Cristina Ferrari, Aurora Kokomani, Iashar Laghai, Riccardo Laudicella, Silvia Migliari, Federica Orsini, Salvatore Antonio Pignata, Cristina Popescu, Erinda Puta, Martina Ricci, Silvia Seghezzi, Alessandro Sindoni, Martina Sollini, Letterio Sturiale, Anna Svyridenka, Vittoria Vergura, Pierpaolo Alongi; Young AIMN Working Group

Federico Caobelli, Department of Nuclear Medicine, Universitätsspital Basel, CH-4032 Basel, Switzerland

Laura Evangelista, Department of Nuclear Medicine, Istituto Oncologico Veneto, 35121 Padua, Italy

Natale Quartuccio, Wolfson Molecular Imaging Centre, University of Manchester, M20 3JJ Manchester, United Kingdom

Demetrio Familiari, Department of Nuclear Medicine, A.R.N.A.S. Garibaldi, 95121 Catania, Italy

Corinna Altini, Cristina Ferrari, Nuclear Medicine Unit, University "Aldo Moro" of Bari, 70121 Bari, Italy

Angelo Castello, Rossella Di Dato, Aurora Kokomani, Iashar Laghai, Vittoria Vergura, Department of Nuclear Medicine, University of Florence, 50121 Florence, Italy

Mariapaola Cucinotta, Department of medical-surgical science and translational medicine, "La Sapienza" University, 00118 Rome, Italy

Riccardo Laudicella, Salvatore Antonio Pignata, Alessandro Sindoni, Letterio Sturiale, Nuclear Medicine Unit, Department of Biomedical Sciences and Morphological and Functional Images, University of Messina, 98121 Messina, Italy

Silvia Migliari, Martina Ricci, Department of Nuclear Medicine, University of Parma, 43121 Parma, Italy

Federica Orsini, Erinda Puta, Department of Nuclear Medicine, University Hospital "Maggiore della Carità di Novara", 28100 Novara, Italy

Cristina Popescu, Department of Nuclear Medicine, Niguarda Ca' Grande Hospital, 20100 Milan, Italy

Silvia Seghezzi, Department of Nuclear Medicine, Hospital of Treviglio, 24047 Treviglio, Italy

Martina Sollini, Humanitas University, Rozzano, 20089 Milan, Italy

Anna Svyridenka, Department of Nuclear Medicine, University of Bologna, 40100 Bologna, Italy

Pierpaolo Alongi, Nuclear Medicine Unit, Department of Radiological Sciences, G. Giglio Institute, 90015 Cefalu, Italy

Author contributions: All authors contributed to the manuscript.

Conflict-of-interest statement: The authors hereby declare that no one of the coworkers has received fees for serving as a speaker, no one holds a position as advisory board member, none has received research funding, no one owns stocks and/or shares in any Companies, no one owns patents.

Data sharing statement: No additional data are available. A formal consent was not obtained due to the nature of the present paper (Review of already published papers).

Manuscript source: Invited manuscript

Correspondence to: Dr. Federico Caobelli, MD, FEBNM, Department of Nuclear Medicine, Universitätsspital Basel, Petersgraben 4, CH-4032 Basel, Switzerland. federico.caobelli@usb.ch

Telephone: +41-61-3286329

Received: March 25, 2016
Peer-review started: March 26, 2016
First decision: May 17, 2016
Revised: June 30, 2016
Accepted: August 27, 2016
Article in press: August 29, 2016
Published online: October 28, 2016

Caobelli F, Evangelista L, Quartuccio N, Familiari D, Altini C, Castello A, Cucinotta M, Di Dato R, Ferrari C, Kokomani A, Laghai I, Laudicella R, Migliari S, Orsini F, Pignata SA, Popescu C, Puta E, Ricci M, Seghezzi S, Sindoni A, Sollini M, Sturiale L, Svyridenka A, Vergura V, Alongi P; Young AIMN Working Group. Role of molecular imaging in the management of patients affected by inflammatory bowel disease: State-of-the-art. *World J Radiol* 2016; 8(10): 829-845 Available from: URL: http://www.wjgnet.com/1949-8470/full/v8/i10/829.htm DOI: http://dx.doi.org/10.4329/wjr.v8.i10.829

Abstract

AIM

To present the current state-of-the art of molecular imaging in the management of patients affected by inflammatory bowel disease (IBD).

METHODS

A systematic review of the literature was performed in order to find important original articles on the role of molecular imaging in the management of patients affected by IBD. The search was updated until February 2016 and limited to articles in English.

RESULTS

Fifty-five original articles were included in this review, highlighting the role of single photon emission tomography and positron emission tomography.

CONCLUSION

To date, molecular imaging represents a useful tool to detect active disease in IBD. However, the available data need to be validated in prospective multicenter studies on larger patient samples.

Key words: White blood cell scintigraphy; Inflammatory bowel disease; Inflammation; ^{18}F-Fluorodehoxiglucose positron emission tomography/computed tomography; Molecular imaging

Core tip: Inflammatory bowel disease (IBD) is a chronic granulomatous inflammatory condition, in which the integrity of the gut epithelium represents a major pathophysiological step. Although endoscopy and barium radiological examinations are the diagnostic "gold standard" for IBD, both techniques require a specific patient preparation, not always feasible or easily tolerated. Molecular imaging with single photon emission tomography and positron emission tomography seems to be a reliable, non-invasive, accurate and easily reproducible diagnostic tool, able to assess location, extent and activity grade of IBD. We here present the current state-of-the art of molecular imaging in the management of patients affected by IBD.

INTRODUCTION

Inflammatory bowel disease (IBD) is a chronic inflammatory condition, in which the integrity of the gut epithelium represents a major pathophysiological step. Both ulcerative colitis (UC) and Crohn's disease (CD) follow a relapsing and remitting course. As such, tools able to diagnose and manage patients affected by these conditions are highly relevant in clinical practice.

Endoscopy and barium radiological examinations are the diagnostic "gold standard" for IBD[1-3]. Unfortunately, both techniques require a specific patient preparation, which is not always feasible and not easily tolerated. Specifically, endoscopy is an invasive procedure associated with increased risk of bowel perforation, if performed during the acute phase of disease[1,3,4]. Moreover, it cannot study the deepest layers of intestinal wall and discover possible extra-intestinal alterations[5]. Finally, in case of CD complicated by strictures, endoscopic exploration often remains incomplete, due to difficulties in going beyond narrowed bowel segments and in exploring the distal side of the strictures[4].

In this context, the need for a novel non-invasive, accurate and easily reproducible diagnostic tool, able to assess location, extent and activity grade of IBD, is crucial[1,6,7]. Molecular imaging with single photon emission tomography (SPECT) and positron emission tomography (PET) seems to be promising, allowing for tracking molecular changes occurring before clinical manifestations.

We therefore aimed at presenting the current state-of-the art of molecular imaging in the management of patients affected by IBD.

MATERIALS AND METHODS

Search strategy

A comprehensive computer literature search of the PubMed/MEDLINE and Web of Knowledge database was performed in order to find important original articles on the role of molecular imaging in the management of patients affected by IBD. Papers on future perspectives in the field and experimental data were also searched. The adopted algorithm was based on a combination of the terms: (a) IBD and (b1) "positron emission tomography" or "PET" or (b2) "single photon emission tomography" or "SPET" and (c1) diagnosis or (c2) prognosis or (c3) follow-up. The search was updated until February 2016 and limited to articles in English. The references of the

retrieved articles were also checked for additional studies as not to exclude possible interesting data.

Article selection

Studies investigating the role of SPECT and PET in patients with IBD were eligible for inclusion. Studies with at least 6 patients were selected. Review articles, articles not in the field of interest, single/double case reports and commentaries were excluded. Meta-analyses were retrieved to provide convincing data for the discussion. Also, abstracts or oral/poster meeting presentations were not included.

RESULTS

Fifty-five original articles were included in this review. Specifically, 10 studies were available on the role of SPECT and 19 on PET. Furthermore, 13 articles were retrieved on the role of molecular imaging in paediatric patients, and 13 articles provided interesting insight on experimental data in the field.

SPECT

Table 1 shows the selected studies on the role of SPECT in adult patients affected by IBD. The majority of the studies were based on the ability of ^{99m}Tc-HMPAO-white blood cell (WBC) to diagnose the presence of IBD. Lachter *et al*[8] showed that ^{99m}Tc-HMPAO-WBC scintigraphy can be useful for patients with CD, while it is not sophisticated for the diagnosis of UC. Some years later, Paredes *et al*[9], reported that patients with suspected recurrent IBD after surgery can be evaluated with ^{99m}Tc-HMPAO-WBC scintigraphy as an alternative to ileoendoscopy. The single-injection technique used for the administration of LeukoScan simplifies the labelling techniques required for white cell imaging. Kerry *et al*[10], investigated ^{99m}Tc-leukoscan and ^{99m}Tc-white cell scan in suspected IBD in 22 patients. Planar ^{99m}Tc-WBC images were acquired at 45 min and 2 h post-injection, while planar ^{99m}Tc-leukoscan images were acquired at 1, 2 and 4 h post-injection and with a SPECT after 4 h. From a head-to-head comparison ^{99m}Tc-WBC scan showed a better diagnostic accuracy in IBD patients than ^{99m}Tc-leukoscan.

A direct comparison between the diagnostic performance of ^{99m}Tc-HMPAO-WBC SPECT and planar images was performed in 2005 and 2011[11,12]. These two studies comprised 22 and 99 patients, respectively and reported comparable results between planar and SPECT images regarding diagnostic accuracy[11,12]. However, SPECT images provided a more detailed visualization of those IBD lesions which were located in critical sites, like terminal ileum (due to the relatively intense overlying background bone marrow activity in the sacro-iliac region), pelvic floor and rectum (because the rectal disease is covered by the intense overlying background activity which is often present in the bladder).

Some authors aimed to quantify the severity of IBD by means of different parameters, like in-house validated scintigraphic indices (SI) at ^{99m}Tc-HMPAO-WBC scan[13] or the stool radioactivity (defined as the disappearance of ^{111}In-radiolabelled leukocytes from the spleen[14] or from the whole body retention[14,15], as they migrates toward regions of inflammation). As a matter of fact, such semi-quantitative methods for the assessment of the severity of disease could be important for an objective evaluation of treatment response, although a more extensive demonstration of their usefulness lacks in the literature.

Van den Brande *et al*[16] investigated whether apoptosis in the intestine underlies the clinical benefit of anti-tumor necrosis factor (TNF) treatment in CD, performing real-time imaging[17,18] of *in vivo* apoptosis by using ^{99m}Tc-annexin V SPECT at baseline and 24 h after Infliximab treatment both in 2 models of murine experimental colitis and in 14 patients with active CD. The authors found a mean increase of 98.7% in colonic uptake of ^{99m}Tc-annexin V in 10 of the 14 responding patients compared with 15.2% in non-responding patients (P = 0.03). Thus, the use of ^{99m}Tc-annexin V SPECT may be envisioned in order to predict the response to Infliximab, given the correlation between the colonic uptake of ^{99m}Tc-annexin V and clinical benefit of anti-TNF treatment. This bears important implications in the choice of the best therapeutic options, also by increasing the cost-effectiveness of Infliximab.

A new emerging radiopharmaceutical agent was investigated to image the presence of Interleukin 8-receptors (IL8-R), which are overexpressed by activated neutrophils into the intestinal wall of patients with IBD. Recently, Aarntzen *et al*[19] evaluated the accuracy of ^{99m}Tc-IL8-R SPECT in a prospective series of patients affected by IBD (15 with CD and 15 affected by UC). Sensitivity and specificity on a per-patient basis for the detection of active disease were 95% and 44% for ^{99m}Tc-IL8-R scan and 71% and 70% for endoscopy, respectively. On a per-segment basis, sensitivity and specificity were 82% and 72% for ^{99m}Tc-IL8-R scan, and 74% and 85% for endoscopy, respectively. The degree of ^{99m}Tc-IL8-R uptake correlated with that of neutrophilic involvement in affected mucosa. As such, the authors showed that ^{99m}Tc-IL8-R SPECT provides a novel imaging technique able to target neutrophil recruitment in the intestinal wall, especially in IBD exacerbations of moderate-to-severe degree. These encouraging results suggest to take advantage from ^{99m}Tc-IL8-R imaging in future studies, as a biomarker to personalize treatment with immunomodulating drugs.

An overview of diagnostic performance of SPECT in the most relevant studies is reported in Table 2.

PET

PET/CT performance in the diagnosis of IBD: Positron emission tomography with ^{18}F-Fluorodehoxiglucose (^{18}F-FDG-PET) fulfills, at least partially, the required criteria for a non-invasive, accurate and easily reproducible diagnostic tool, able to assess location, extent and activity degree of IBD. Inflamed tissues, especially during the active phase of disease, are often characterized by a high uptake of ^{18}F-FDG on PET

Table 1 Studies on planar scintigraphy and single photon emission tomography included in the present review

Ref.	Year of pub	Journal	*n* of pts	Indication	Imaging technique	Gold standard	Conclusion
Rowe *et al*[14]	1995	*Am J Gastroenterol*	11	The measurement of the severity colitis	^{111}In-labelled leukocyte planar scintigraphy	Truelove and Witts criteria	The disappearance of radioactivity from the spleen or whole body during 24 h is likely to be a useful and accurate index of disease severity in inflammatory colitis Scintigraphy is useful for patients with CD, but not for ulcerative colitis. Leukocyte scintigraphy is more useful for the reassessment than initial diagnosis (particularly in case of structuring and fistulising CD). ^{99m}Tc-Leukoscan cannot be useful for the evaluation of IBD
Lachter *et al*[8]	2003	*Hepato-Gastroenterology*	46	Diagnosis of suspected inflammatory bowel disease	^{99m}Tc-HMPAO planar scintigraphy	Histology	
Kerry *et al*[10]	2005	*Nuclear Medicine Communication*	22	Diagnosis of IBD and comparison between ^{99m}Tc-HMPAO and ^{99m}Tc-Leukoscan	^{99m}Tc-HMPAO planar scintigraphy ^{99m}Tc-Leukoscan planar scintigraphy ^{99m}Tc-Leukoscan SPECT	Histology Radiology Response to treatment	
Biancone *et al*[11]	2005	*Am J Gastroenterol*	22	Comparison between ^{99m}Tc-HMPAO planar and SPECT for the assessment of intestinal infiltration in CD	^{99m}Tc-HMPAO planar and SPECT	Histology	SPECT images may better discriminate between intestinal and bone marrow uptake, thus allowing a better visualization of CD lesions in the pelvis (especially for perianal and enterovesical disease)
Cheow *et al*[15]	2005	*Eur J Nucl Med Mol Imaging*	30	To quantify disease activity in IBD	^{99m}Tc-granulocytes planar scintigraphy and ^{111}In-granulocytes	NA	A dedicated whole-body counting using ^{111}In can be useful to quantify inflammatory disease, especially IBD
Van den Brande *et al*[16]	2007	*Gut*	14	To predict the efficacy of anti-TNF treatment in IBD	^{99m}Tc-annexin V	Histology	The uptake of ^{99m}Tc-annexin V correlates with clinical benefit of anti-TNF treatment
Mota *et al*[13]	2010	*World J Gastroenterol*	20	To evaluate inflammatory activity in CD patients	^{99m}Tc-HMPAO	NA	Scintigraphy with radiolabeled HMPAO could be useful for the evaluation of intestinal activity in CD
Paredes *et al*[9]	2010	*Journal of Crohn's and Colitis*	40	To assess the accuracy of abdominal ultrasonography, ^{99m}Tc-HMPAO in recurrent CD	^{99m}Tc-HMPAO	Histology	^{99m}Tc-HMPAO can be used in case of postsurgical recurrence in CD, in particular for those patients who reject endoscopic examination or for the assessment of neoterminal ileum
Hillel *et al*[12]	2011	*Nuclear Medicine Communication*	99	To compare planar and SPECT imaging in IBD	^{99m}Tc-HMPAO	NA	SPECT improves interoperator variability and probably sensitivity for IBD. The size of lesion suggest that planar images underestimates the extent of active disease
Aarntzen *et al*[19]	2015	*J Nucl Med*	30	To assess the accuracy of ^{99m}Tc-CXCL8 SPECT to detect and to localize disease activity	^{99m}Tc-CXCL8	Histology	^{99m}Tc-CXCL8 is a novel target for neutrophil recruitment to the intestinal wall, especially in moderate to severe exacerbations of IBD

CD: Crohn's disease; IBD: Inflammatory bowel disease; TNF: Tumor necrosis factor; NA: Not available; SPECT: Single photon emission tomography; pts: Patients.

images, due to overexpression of glucose transporters on the surface of neutrophils and macrophage. The relatively recent addition of computed tomography (CT) to ^{18}F-FDG-PET scan allows to simultaneously analyze functional and morphologic aspects of disease, thus permitting discriminating between active and quiescent inflammation (Figure 1). Moreover, other complications such as abscesses, fistulas, inflamed lymph nodes can be effectively detected[1-4,6,7,20,21].

In the latest 10 years, a handful of studies explored the role of ^{18}F-FDG-PET, eventually fused with CT, in the evaluation of disease activity in patients with known IBD.

Table 2 Diagnostic accuracies in some selected studies on single photon emission tomography

Ref.	Year of pub	Tracer	Sensitivity	Specificity
Lachter *et al*[8]	2003	^{99m}Tc-HMPAO	58%	100%
Kerry *et al*[10]	2005			
^{99m}Tc-HMPAO (2 h)		^{99m}Tc-HMPAO	87%	86%
^{99m}Tc-Leukoscan (1 h)		^{99m}Tc-Leukoscan	20%	86%
^{99m}Tc-Leukoscan (2 h)			40%	100%
^{99m}Tc-Leukoscan (4 h)			73%	57%
^{99m}Tc-Leukoscan (4 h-SPECT)			87%	57%
Paredes *et al*[9]	2010	^{99m}Tc-HMPAO		
Endoscopic recurrence			88%	42.9%
Scintigraphic recurrence			73.3%	88.2%
Aarntzen *et al*[19]	2015	^{99m}Tc-CXCL8	95%	44%

SPECT: Single photon emission tomography.

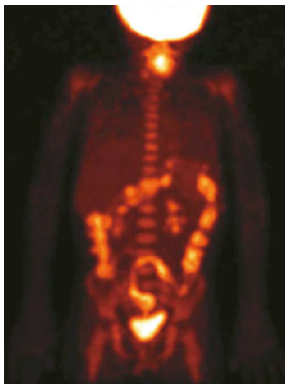

Figure 1 Maximum intensity projection image of an positron emission tomography with ^{18}F-Fluorodehoxiglucose examination shows diffuse and intense radiopharmaceutical uptake in the large bowel. Reprinted with permission of Springer Verlag from Cistaro *et al*.

In 2007 Meisner *et al*[6] published the first prospective study on 12 patients with known and at least moderate IBD (7 UC and 5 CD) undergoing ^{18}F-FDG-PET/CT. In this pilot-study, the correlation between active regions on PET scan and those found to be active based on clinical criteria (including colonoscopy and radiologic examinations results) was equal to 95.8% in UC and 81.3% in CD patients. Interestingly, the co-registration with CT was helpful for anatomical identification of different bowel segments in CD, especially in case of small bowel involvement and surgically treated patients, whereas PET alone considered adequate to accurately define anatomic regions in those patients diagnosed with UC.

One of the main limits of ^{18}F-FDG-PET is represented by false positive cases due to physiologic uptake of the radiopharmaceutical in normal bowel, caused by the typically high turnover of intestinal mucosa, the presence of material in the lumen, bacterial flora, lymphoid tissue inside the mucosa, but mostly by the peristaltic activity of muscular layer and the physiologic collapse of bowel loops. However, these two latter factors can be effectively overcome by a proper distention of bowel segments through the administration of great amount of fluids, as in the case of PET/CT enterography[1,3,7,20,21]. To reduce the number of false positive findings in the intestinal tract during a PET scan, Franquet *et al*[22] proposed to undertake a therapy with Rifaximine 2 d before the PET scan. In their paper, this patient preparation allowed to reduce the unspecific FDG uptake.

For the evaluation of patients with CD, Ahmadi *et al*[7] retrospectively studied 41 patients with known or suspected active disease of the small bowel, who underwent ^{18}F-FDG-PET/CT enterography. Thirty patients presented a total of 48 pathological bowel segments on CT enterography, of which 38 (79%) also showed an abnormal ^{18}F-FDG uptake. All pathological areas identified by ^{18}F-FDG-PET/CT enterography corresponded to abnormal areas visualized on CT enterography. CT enterography score of activity and semi-quantitative PET parameters showed also a significant correlation (P = 0.03). In a prospective study Groshar *et al*[20] also explored the ability of ^{18}F-FDG-PET to detect IBD and to assess its degree of activity. The authors compared ^{18}F-FDG-PET to enterography in 28 patients with known or suspected active CD. Eighty-five abnormal segments were found in 22 patients, while the remaining 6 subjects had unremarkable finding both on PET and CT enterography. The authors found a significant difference in abnormal and normal segments in mean wall thickness, mean mural enhancement and maximum standardized uptake value (SUV_{max}, $P < 0.0001$). A good correlation was also found between SUV_{max} and wall thickness or mural enhancement measurements, both in the colon and ileum ($P < 0.00001$). SUV_{max} correlated well also with the grade of other CT enterography parameters used to detect active inflammation, such as parietal attenuation, perienteric fat attenuation and perienteric/pericolic hypervascularization ($P < 0.001$).

A pilot study also analyzed the diagnostic advantage of adding ^{18}F-FDG-PET to CT enterography[21]. The authors compared PET and CT enterography alone in 13 CD patients with clinically suspected active disease, using histology after surgery or biopsy performed during endoscopy as gold standard (in 6 and 7 patients, respectively). In 3 (23%) patients, ^{18}F-FDG-PET allowed

to identify signs of active disease otherwise missed by CT enterography alone, including an entero-colic fistula in one patient. Both techniques were able to identify all bowel segments with at least a moderate activity. There was a significant correlation between both techniques and histology in the evaluation of disease activity.

In a prospective study, Das *et al*[1] compared ^{18}F-FDG-PET/CT and colonoscopy in 15 patients, affected by mild to moderate UC. ^{18}F-FDG-PET/CT detected 66 involved bowel segments, whereas colonoscopy found 67 pathological regions, so that the detection rate of ^{18}F-FDG-PET/CT was 98.5% compared to colonoscopy. A significant correlation between the two techniques was also found in the definition of disease extent (κ = 55.3%, P = 0.02).

^{18}F-FDG-PET was also compared to other imaging techniques, showing in many cases even better diagnostic performance. In 2012 Holtmann *et al*[2] evaluated 43 patients with active CD, undergoing ^{18}F-FDG-PET, ileo-colonoscopy and hydro-magnetic resonance imaging (MRI). A total of 241 bowel segments in the terminal ileum and colon were examined. Endoscopy detected inflammation in 80 of 241, while ^{18}F-FDG-PET in 72 (sensitivity and a specificity of 90% and 92.6%, respectively). Conversely, hydro-MRI identified 53/80 inflamed segments with a sensitivity of only 66.3% and a specificity of 99.4%. Specifically, hydro-MRI displayed the lowest sensitivity but a 100% specificity for all colon segments, while in the terminal ileum sensitivity and specificity were 100% and 93.3%, respectively (*vs* 86.4% and 93.3%, respectively, of ^{18}F-FDG-PET). In the proximal ileum, ^{18}F-FDG-PET and hydro-MRI had the same results in all cases, reaching identical sensitivity and specificity.

One of the main issues in CD patients is to distinguish the nature of strictures (predominantly inflammatory or fibrotic, or mixed), as they represent a common complication of CD and show a very high rate of recurrence after surgical resection. As such, it is crucial to discriminate those lesions likely to benefit from surgical treatment (the predominantly fibrotic ones) from those still medically treatable (the inflammatory ones). With this regard, some authors suggested a possible role for ^{18}F-FDG-PET, although data are still limited and controversial[2,4,5]. While Shyn and colleagues reported no significant difference in SUV_{max} between the strictures deserving or not a surgical resection, although in a small patient sample[21], Holtmann *et al*[2] showed that both hydro-MRI and ^{18}F-FDG-PET have very high accuracy in detecting and characterizing strictures.

Louis *et al*[23] prospectively studied 22 patients with CD. Ninety-five ileal segments were comparatively analyzed by endoscopy and ^{18}F-FDG-PET/CT, showing a significant correlation between CD endoscopic index (CDEI) and $RSUV_{max}$ (the ratios of each positive-segment SUV_{max} over the SUV_{max} of the liver). In their paper, ^{18}F-FDG-PET/CT detected and localized the vast majority of gastrointestinal segments with moderate to severe lesions (sensitivity for superficial ulcers, deep ulcers, and strictures was 84.4%), allowing a non-invasive evaluation of the ongoing pathologic process in the gastrointestinal tract. Overall, ^{18}F-FDG-PET/CT detected 35 of 48 endoscopically affected segments (sensitivity for the detection of endoscopic lesions 72.9%). This study demonstrated an important role of PET/CT in detecting active intestinal disease beyond the mucosa. This ability is important because complications of CD such as strictures may develop despite the lack of mucosal lesions visible at endoscopy, and because the presence of extraenteric inflammation is widely recognized as an important prognostic factor in CD.

PET/CT enteroclysis has been suggested in several studies as a new promising approach. This technique essentially consists in a simple extension of CT enteroclysis and provides information both on morphological details and on the metabolic activity of the lesion(s). In a study by Das *et al*[24], PET/CT enteroclysis, as a single test, detected involvement of a significantly higher number of intestinal segments [total = 50, 23 in the small intestine and 27 in the large intestine, (P < 0.01) compared to conventional barium studies (16 segments of small intestine)] and colonoscopy (17 segments of large intestine). Similarly, a prospective study by Lenze *et al*[4] compared the performance of ^{18}F-FDG-PET/CT enteroclysis, MR enteroclysis and trans-abdominal ultrasound in the detection of CD strictures and in the differentiation of fibrotic *vs* inflammatory ones, using invasive endoscopy and histology as reference. In 30 symptomatic patients endoscopy detected 37 strictures, both PET/CT enteroclysis and MR enteroclysis 30/37 (81%) and ultrasound 25/37 (68%). By combining two methods, the sensitivity increased: Specifically, it was reported to be 92% when combining PET/CT and ultrasound and 89% when combining MR and ultrasound or MR and PET/CT. However, the differentiation rates of the strictures nature was low and equal to 57% for MR, 53% for PET/CT and 40% for ultrasound. Considering only inflammatory strictures, MR and PET/CT correctly classified 94% and 83% of them, respectively, *vs* 66% depicted by ultrasound. By combining two methods (MR and ultrasound or PET/CT with ultrasound), all the strictures deserving surgical resection could be identified.

More recently, a retrospective study of Catalano *et al*[5] investigated the role of ^{18}F-FDG-PET/MR enterography in discriminating between inflammatory and fibrotic strictures associated with CD, by using "quantitative" methods. Nineteen patients surgically treated within one month from imaging were evaluated and the following parameters were recorded for each resected bowel segment: The "SI" on T2 weighted sequences, the "apparent diffusion coefficient (ADC)", the SUV_{max} and the values obtained by multiplying the first two parameters by SUV_{max} (SI × SUV_{max} and ADC × SUV_{max}, respectively). In the 19 patients evaluated, 33 strictured bowel segments were resected. Of these, 7 presented with predominant inflammation, 11 with predominant fibrosis and 15 with a mixed pattern. A significant difference among these three types of stricture was reported in SUV_{max} (P

< 0.03), SI × SUV_{max} (P = 0.046) and ADC × SUV_{max} (P = 0.044), but not in SI and ADC. The most accurate biomarker in discriminating fibrotic from inflammatory strictures was ADC × SUV_{max}, with a cut-off < 3000 (mean accuracy = 0.71), followed by SUV_{max} < 2.5 (mean accuracy = 0.67). The other quantitative biomarkers tested (SI × SUV_{max} < 2000, SI < 750, ADC < 1200 × 10^{-3} mm^2/s) showed suboptimal performance (accuracy = 0.63, 0.48 and 0.54, respectively). The selected studies and the most relevant findings are displayed in Tables 3 and 4.

Therapy response and disease monitoring: Spier *et al*[25] reported higher FDG uptake in patients with clinically active disease (CD-activity index > 150 or UC-activity index > 6) than in those with inactive disease. This study suggests that FDG PET may be useful in identifying active inflammation in IBD as well as in the long-term monitoring. Glaudemans *et al*[26] reported a good correlation between clinical symptoms and PET/CT findings in a small cohort of subjects with moderately active IBD (n = 5) undergoing FDG PET/CT before and after successful medical therapy.

Rubin *et al*[27] evaluated a cohort of ten patients with UC in a strictly defined remission state (at least six month). A total body PET/CT was performed. The bowel was divided in several areas of interest and the uptake of FDG was scored on 3 point scale compared to the liver uptake. PET/CT showed 90% specificity in assessing disease activity in UC quiescent patients, and allowed the choice of the most adequate therapy options. Interestingly, PET could identify residual inflammatory activity in the colon despite negative endoscopic, histologic, and clinical findings.

Lapp *et al*[28] demonstrated that PET/CT significantly aids in the clinical decision-making in selected patients with known or suspected IBD. In their paper, although used in a heterogeneous group of patients (four with CD, two with pouches, and one without IBD), PET/CT could effectively lead to the choice of an appropriate therapy in each patient and proved superior to currently available modalities (*e.g.,* laboratory, CT, endoscopy). Jacene *et al*[29] determined single-pixel maximum standardized uptake value corrected for lean body mass (SUL_{max}) on PET/CT for lesions potentially representing active bowel inflammation. Patients with severe chronic inflammation had significantly higher SUL_{max} than those with mild or moderate chronic inflammation. Semiquantitative analyses of ^{18}F-FDG uptake helped in distinguishing predominantly active inflammation from fibrotic strictures and muscle hypertrophy. Specifically, a SUL_{max} cutoff of 8 seemed to represent the most accurate threshold. Interestingly, patients with predominantly active inflammation, underwent surgery closer to the time of PET/CT compared with those with predominantly fibrosis or muscle hypertrophy. This information may be helpful for referring gastroenterologists considering surgery *vs* medical therapy for patients with CD who present with obstructive symptoms.

In several papers, PET/CT was reported to be superior to other standard radiologic or endoscopic pouch evaluations in the assessment of the response to treatment. Kuwaki *et al*[30] investigated 12 patients with CD undergoing granulocyte/monocyte apheresis (GMA). The response to treatment was monitored by measuring standard laboratory tests, CD activity index (CDAI) score, International Organization for the Study of Inflammatory Bowel Diseases score and regional and global bowel uptake on FDG-PET (baseline, at the 5th and at the 10th session of GMA). In 6 of 12 patients, a significant correlation was found between clinical and CDAI improvement and FDG uptake reduction *vs* baseline scan. As such, longitudinal changes in FDG-PET uptake in the involved bowel areas is of potential clinical value for assessing both regional and global bowel disease activity in CD patients during GMA therapy.

Other semiquantitative parameters of FDG PET/CT were investigated by Saboury *et al*[31] in order to determine the feasibility and potential clinical utility of this technique in the assessment of therapy response in CD. In a cohort of 22 subjects with CD in treatment undergoing ^{18}F-FDG-PET followed by ileocolonscopy and laboratory assay of Fecal Calprotectine and C-reactive protein (CRP), the authors searched for correlation between the global PET quantification measure (GCDAS, global SUVs) with CDAI, fecal calprotectin, CDEIs, and CRP level. A significant correlation was demonstrated between SUV_{max}, PVC-SUV_{mean}, and PVC-TLG and CDEIS. Similarly, GCDAS was significantly correlated with CDAI and fecal calprotectin. As such, disease activity was effectively monitored through these semiquantitative parameters, allowing for a tailored treatment.

Molecular imaging in paediatrics

An overview of the selected studies on molecular imaging in paediatric patients is shown in Table 5.

Diagnosis: Planar scintigraphy and SPECT: As for adult patients, leukocyte-labelled scintigraphy is a useful tool in the diagnosis and therapeutic strategy of IBD, providing information on the presence, the activity and the extent of the disease, particularly in the terminal ileum[32]. Charron *et al*[33] reported a large series of paediatric IBD patients evaluated by ^{99m}Tc-HMPAO-WBC scintigraphy. One hundred and thirty-two patients with IBD were included, along with 52 patients with nonspecific gastrointestinal symptoms and a low probability of IBD and 31 healthy controls. Images were analysed considering bowel activity in 8 segments and scored using a 6-point scale based on liver, spleen and bone marrow uptake. ^{99m}Tc-HMPAO-WBC scintigraphy was proven useful in assessing the extent and distribution of inflammation [sensitivity 90%, specificity 97%, positive predictive value (PPV) 97%, negative predictive value (NPV) 93%, overall accuracy 93%]. Caobelli *et al*[34] found a correspondence between severity of inflammation as assessed by means of Mayo Score and uptake intensity (Scan Activity Index) in 87%

Table 3 Overview of the selected studies on the role of positron emission tomography in diagnosing inflammatory bowel disease

Ref.	Year of pub	Journal	*n* of pts	Indication	Imaging technique	Gold standard	Conclusions
Meisner *et al*[6]	2007	*Inflamm Bowel Dis*	12	To identify regions of active inflammation in patients with known and at least moderate UC or CD	^{18}F-FDG-PET/CT	Clinical evaluation including colonoscopy and radiologic imaging	There is high correlation between ^{18}F-FDG-PET activity and clinical disease activity CT is necessary for anatomical identification of different bowel segments in CD patients with small bowel involvement or surgically treated
Das *et al*[1]	2010	*Eur J Nucl Med Mol Imaging*	15	To assess the extent and severity of disease in patients with active, mild to moderate UC	^{18}F-FDG-PET/CT colonography	Colonoscopy	^{18}F-FDG-PET/CT colonography is a useful tool for the assessment of extent and activity of UC
Ahmadi *et al*[7]	2010	*Inflamm Bowel Dis*	41	To identify disease activity in patients with known or suspected active CD of the small intestine To find out possible risk factors for therapy failure	Localized 18F-FDG-PET/CTe	NA	^{18}F-FDG-PET scan does not increase CTe in detection of active disease A low ^{18}F-FDG uptake in at least one small bowel segment, resulted to be pathological on CTe, represent a risk factor for medical treatment failure
Groshar *et al*[20]	2010	*J Nucl Med*	28	To evaluate disease activity in patients with known or suspected active CD	^{18}F-FDG-PET/CTe	NA	SUV_{max} correlates well with CTe findings of active disease. It might be a reliable objective method for quantifying CD's activity
Shyn *et al*[21]	2010	*J Nucl Med*	13	To detect active disease and assess severity of inflammation in patients with clinically suspected active CD	^{18}F-FDG-PET/CTe	Histology after surgery or after biopsy performed during endoscopy	^{18}F-FDG-PET added to CTe may improve the detection of active disease
Holtmann *et al*[2]	2012	*Dig Dis Sci*	43	To detect bowel segments with active CD	18F-FDG-PET	Endoscopy for distal ileum and colon, hydro-MRI for proximal ileum	^{18}F-FDG-PET diagnostic performance in the detection of bowel segments with active disease is high. Compared to ^{18}F-FDG-PET, hydro-MRI shows much lower sensitivity but higher specificity for all colon segments, higher sensitivity and the same specificity for terminal ileum and same performance for proximal ileum. Both methods seem to have high accuracy in strictures detection and characterization of their nature
Lenze *et al*[4]	2012	*Inflamm Bowel Dis*	30	To detect CD strictures and differentiate inflammatory from fibrotic ones	18F-FDG-PET/CT enteroclysis, MR enteroclysis, transabdominal ultrasound	Endoscopy + hystology	All the three studied techniques have good strictures detection rates relating to the gold standard, but none of them can accurately differentiate strictures' nature. However, a combination of methods allows the detection of all strictures requiring surgery
Catalano *et al*[5]	2016	*Radiology*	19	To differentiate fibrotic from inflammatory strictures in CD patients	18F-FDG-PET/MR enterography	Post-surgical histology	^{18}F-FDG-PET/MR enterography offers valid biomarkers for stricture evaluation

SPECT: Single photon emission tomography; CD: Crohn's disease; UC: Ulcerative colitis; NA: Not available; ^{18}F-FDG-PET: Positron emission tomography with ^{18}F-Fluorodehoxiglucose; CT: Computed tomography; MRI: Magnetic resonance imaging; SUV: Standardized uptake value; CTe: CT esensitivity; pts: Patients.

of patients and a full correspondence of location and severity of lesions in 15/16 patients. Overall, reported sensitivity and specificity for ^{99m}Tc-HMPAO-WBC scintigraphy were 94% and 86%, respectively. On the other hand, other authors found a good correlation between scintigraphy and endoscopy for the intensity of inflammation (r = 0.70) but a poor correlation regarding the number of involved segments (r = 0.30), due to a significantly higher sensitivity of endoscopy as compared with scintigraphy[35]. ^{99m}Tc-HMPAO-WBC scintigraphy may distinguish discontinuous from continuous colitis with very good results[36].

Table 4 Diagnostic accuracies in some selected studies on positron emission tomography

Ref.	Year of pub	Tracer	Sensitivity	Specificity
Meisner *et al*[6]	2007	^{18}F-FDG		
UC			95.8%	NA
CD			81.3%	NA
Das *et al*[1]	2010	^{18}F-FDG	98.5%	NA
Ahmadi *et al*[7]	2010	^{18}F-FDG	NA	NA
Groshar *et al*[20]	2010	^{18}F-FDG	NA	NA
Shyn *et al*[21]	2010	^{18}F-FDG		
Detection of bowel segments with active CD				
Using a threshold > 1 (at least mild activity)			63.3%	100%
Using a threshold > 2 (at least moderate activity)			100%	89.7%
Holtmann *et al*[2]	2012	^{18}F-FDG		
Detection of active CD				
In the terminal ileum + colon (on a per segment-based analysis)			90%	92.6%
In the proximal ileum (on a per patient-based analysis)			100%	100%
Lenze *et al*[4]	2012	^{18}F-FDG		
Detection of CD strictures			81%	NA
Differentiation of the nature of				
All strictures			53%	
Only inflammatory ones			83%	
Only fibromatous ones			11%	
Only mixed ones			0%	
Treglia *et al*[65] (meta-analysis) (on a per segment-based analysis)	2013	^{18}F-FDG	85%	87%
Zhang *et al*[3] (meta-analysis)	2014	^{18}F-FDG, ^{99m}Tc-HMPAO,		
^{18}F-FDG		^{99m}Tc-monoclonal		
On per-bowel-segment basis		antigranulocyteantibody	0.84	0.86
On per-patient basis			0.59	1
^{99m}Tc-HMPAO			0.86	0.50
On per-bowel-segment basis			0.79	0.76
On per-patient basis			0.91	0.85
^{99m}Tc-monoclonal antigranulocyte antibody on per-bowel-segment basis			0.45	0.94
Catalano *et al*[5]	2016	^{18}F-FDG	(Mean)	(Mean)
Detection of fibrotic CD strictures by				
ADC × SUV_{max} < 3000			0.67	0.73
SI on T2-weightedimages × SUV_{max} < 2000			0.77	0.57
SUV_{max} < 2.5			0.79	0.61
ADC < 1250 × 10^{-3} mm^2/s			0.84	0.26
SI on T2-weightedimages < 750			0.73	0.13

SPECT: Single photon emission tomography; CD: Crohn's disease; UC: Ulcerative colitis; NA: Not available; ^{18}F-FDG: ^{18}F-Fluorodehoxiglucose; SUV: Standardized uptake value; ADC: Apparent diffusion coefficient; SI: Scintigraphic indices.

The use of ^{99m}Tc-HMPAO-WBC scan as initial screening modality to exclude IBD has been suggested, although controversial results have been reported. While a study showed that ^{99m}Tc-HMPAO-WBC scintigraphy is more sensitive than upper gastrointestinal small bowel follow-through (SBFT)[37], other authors stated that ^{99m}Tc-HMPAO-WBC scintigraphy should not be depended upon as a screening test for CD, since its performance compares unfavourably with each of the conventional investigative techniques[38,39].

Few data are available on other tracers. Peacock *et al*[40] reported good results using ^{99m}Tc-Stannous colloid WBC scintigraphy (88% sensitivity, 90% specificity) although agreement was poor for topographic localization of disease when compared to conventional imaging. However, due to a non-inferiority principle (results at least comparable to those of other WBC tracers) authors concluded that in children, ^{99m}Tc-stannous colloid WBC scintigraphy should be preferred in view of lower cost, shorter preparation time, and smaller blood volumes required.

Bruno *et al*[41] reported a higher sensitivity of immunoscintigraphy in CD than in UC (94% and 85%, respectively), although specificity was suboptimal in identifying clinical remission during follow-up. In fact, scintigraphy resulted positive during clinical remission in 73% of patients with CD and in 66.7% of patients with UC.

Diagnosis: PET: The paediatric literature studying the value of ^{18}F-FDG-PET and ^{18}F-FDG-PET/CT in IBD is limited, heterogeneous, and mostly restricted to retrospective studies.

One of the first article (published in 1999) was a retrospective study performed by Skehan *et al*[18]. The authors included 25 young patients with suspected IBD who had undergone ^{18}F-FDG-PET scan and colonoscopy with multiple biopsies, SBFT or both, which were used as a reference standard. ^{18}F-FDG-PET uptake in the gut was considered pathological if greater than that of the vertebral spine. ^{18}F-FDG-PET showed a per-patient sensitivity and specificity of 81% and 85%, respectively. On a segment-by-segment basis, PET correctly identified

Table 5 Studies on molecular imaging in paediatric patients included in the present review

Ref.	Year	Pts (*n*)	Age (range)	Type of study	Clinical setting	Principal results	Technique	Segments evaluated (*n*)	Criterion for positivity
Papós *et al*[48]	1996	20	4-18	Prospective	IBD	sensitivity, specificity, and accuracy of LS were 93%, 88% and 91%, respectively	^{99m}Tc-HMPAO-WBC planar scintigraphy (30 min and 2 and 3 h)		Scored relative to the normal bone marrow uptake (0, no uptake; 1 < bone marrow uptake; 2 = bone marrow uptake; and 3 > bone marrow uptake)
Charron *et al*[36]	1998	178	n.r.	Retrospective		Useful in distinguishing discontinuous from continuous colitis	^{99m}Tc-HMPAO-WBC planar scintigraphy + SPECT (0.5-1 h, 2-4 h)		
Cucchiara *et al*[35]	1999	48	2-17	Prospective	suspected IBD	significant correlation between results of scintigraphy and endoscopy for the intensity of inflammation	^{99m}Tc-HMPAO-WBC planar scintigraphy (dynamic + 30, 60, 120 and 180 min)	9	Abnormal if activity was seen in the gut within the first hour. 0 = no labeling; 1 = less than bone marrow; 2 = greater than bone marrow, less than liver; and 3 = greater than or equal to liver
Del Rosario *et al*[50]	1999	35	2-20	Retrospective	IBD	83% sensitivity which prompted more aggressive management in 75% of cases	^{99m}Tc-HMPAO-WBC planar scintigraphy (30 min + 2 h)		
Charron *et al*[33]	1999	184	n.r.	Retrospective		Sensitivity = 90%, specificity = 97%, overall accuracy = 93%	^{99m}Tc-HMPAO-WBC planar scintigraphy + SPECT (0.5-1 h, 2-4 h ± 6 h ± 24 h)		
Charron *et al*[37]	2000	262	n.r.	Retrospective	IBD	Useful as initial screening modality to exclude IBD	^{99m}Tc-HMPAO-WBC planar scintigraphy + SPECT (0.5-1 h, 2-4 h)		
Alberini *et al*[32]	2001	28	2-15	Retrospective		Sensitivity and specificity were 75% and 92% for ^{99m}Tc-HMPAO-WBC	^{99m}Tc-HMPAO-WBC planar scintigraphy (1 + 3 h, p.i.)		
Davison *et al*[38]	2001	10	n.r.	Prosepctive	CD	^{99m}Tc-HMPAO leucocyte scintigraphy should not be depended upon as a screening test for Crohn's disease	^{99m}Tc-HMPAO-WBC planar scintigraphy + (45 min + 3.5 h)		Abdominal isotope uptake equal to or greater than that associated with the bone marrow was considered to indicate significant inflammation
Bruno *et al*[41]	2002	66	4-19	Prospective		Sensitivity of immunoscitigraphy was 94% for CD and 85% for UC with a relative low specificity	99mTc-BW250/183 planar scintigraphy (4 + 24 h, p.i.)		
Grahnquist *et al*[39]	2003	95	2-16	Prospective	Suspected IBD (screening test)	As a screening test for children with suspected IBD the calculated sensitivity was 75%, and the specificity was 82%	^{99m}Tc-HMPAO-WBC planar scintigraphy (45 min + 3.5 h)	6	
Peacock *et al*[40]	2004	64	2-19	Retrospective	Suspected IBD	^{99m}Tc-Stannous colloid LS had an 88% sensitivity, 90% specificity	^{99m}Tc-stannous colloid WCS planar + SPECT (1 h, 3 h)		
Chroustova *et al*[47]	2009	40	5-18		Monitoring IBD (17 = UC, 23 = CD)	^{99m}Tc-HMPAO-WBC provided good information about the current stage of disease in IBD monitoring	^{99m}Tc-HMPAO-WBC planar scintigraphy + SPECT (30-45 min, 2 h, 3 h)		Graded 1-3 according to the uptake intensity. Grade 1 = a barely detectable abnormal uptake, grade 3 = an abnormal uptake at least as intense as that in the bone marrow and grade 2 was between these extremes. The extent of the abnormal uptake was subjectively classified as A (restricted to a single small focus), C (diffuse, such as in pancolitis) or B (between these extremes)
Caobelli *et al*[34]	2011	52	2-17	Prospective		Sensitivity of 94%, specificity of 86%, and negative predictive value of 96% to diagnose IBD. During the follow-up, all relapses and remissions were correctly recognized	^{99m}Tc-HMPAO-WBC planar scintigraphy (0.5 h, 3 h, p.i.)		Disease severity was graded by the focal uptake intensity *vs* iliac bone uptake (Scan Activity Index) and compared with Endoscopy Mayo Score

SPECT: Single photon emission tomography; CD: Crohn's disease; UC: Ulcerative colitis; IBD: Inflammatory bowel disease; WBC: White blood cell; LS: Leukocyte scintigraphy; pts: Patients.

the presence/absence of active disease in 60 of 79 (76%) bowel segments (sensitivity and specificity were 71% and 81%, respectively).

In 2005 Lemberg *et al*[42] published a prospective study including 65 children with newly diagnosed IBD (37/65 patients), with symptoms suggestive to recurrent disease (18/65 patients) or with recurrent abdominal pain (10/65 patients). ^{18}F-FDG-PET scan results were compared with SBFT, pneumocolon and/or colonoscopy and demonstrated a per-patient sensitivity in UC (n = 17), CD (n = 38) and recurrent abdominal pain of 76%, 82% and 100%, respectively. The specificity of ^{18}F-FDG-PET *vs* SBFT was 100% both for UC and CD, while it was 50% for CD and 81% for UC if compared to colonoscopy. The authors concluded that, although PET may not be able to replace conventional studies, it may be useful in case of difficult performance or failing of conventional studies. Additionally, Löffler *et al*[43] studied 23 children with suspected IBD in a retrospective study, comparing ^{18}F-FDG-PET to endoscopy with biopsies and abdominal ultrasound. Inflammation was graded for each bowel segment on a 3-point scale, namely not inflamed, minimally inflamed and moderately-to-severely inflamed. ^{18}F-FDG-PET scans were analysed semi-quantitatively calculating SUV for all bowel segments, normalized to that of the liver. A score $\geqslant$ 3 or a SUV_{max}/SUV_{liver} ratio > 1.2 was considered positive for inflammation. ^{18}F-FDG-PET showed higher sensitivity (98%) but lower specificity compared both to ultrasound (56% *vs* 92%) and to endoscopy (90% *vs* 75%). However, ^{18}F-FDG-PET proved to be more reliable when assessing small bowel involvement (sensitivity = 100%; specificity = 86%; accuracy = 90%).

More recently, Däbritz *et al*[44] compared results of PET/CT to conventional diagnostic procedures on a segment-based analysis. An FDG uptake in the gut greater than that of the liver was considered pathological. Following these criteria, ^{18}F-FDG-PET/CT showed per-patient sensitivity and specificity of 97% and 100%, respectively, and per-segment sensitivity and specificity of 82% and 97%, respectively (PPV 96%, NPV 88%, accuracy 91%). Berthold *et al*[45] retrospectively analysed 23 young symptomatic patients undergoing endoscopies (gastroscopy and colonoscopy) with biopsies, MRI and ^{18}F-FDG-PET, eventually fused with CT, as part of the diagnostic workup. Positive PET findings were defined as a diffuse and clearly increased FDG uptake in the bowel. In this study, sensitivity and specificity of ^{18}F-FDG-PET was 25% and 100% in the stomach and duodenum, 74% and 88% in the colon and 89% and 75% in the terminal ileum. Especially interesting was the diagnostic performance in assessing lesions involving terminal ileum, for which ^{18}F-FDG-PET appears to be a reliable tool able for the non-invasive assessment of the presence and extent of the disease.

Follow-up: Only a few studies about paediatric patients have been published and are characterized by a smaller number of patients compared to those performed in adults and by the lack of an adequately long follow-up[46]. Chroustova *et al*[47] reported that ^{99m}Tc-HMPAO-WBC scintigraphy may play an important role in the follow-up of patients with IBD if the findings are evaluated in conjunction with clinical symptoms and laboratory examinations, providing good information about the current stage of disease. Similar results were replicated by Papós *et al*[48], wherein the patient activity index scores (sum of the activity scores as measured in each bowel segment) were compared with laboratory parameters. The scintigraphic activity index showed an excellent correlation with several important activity markers in IBD, such as CRP, α2 globulin, iron, and erythrocyte sedimentation rate. Some impressive cases have been reported, in which ^{99m}Tc-HMPAO-WBC scintigraphy could effectively trace the changing in disease activity over time in paediatrics (Figure 2).

However, despite some advantages of ^{99m}Tc-HMPAO-WBC scintigraphy over conventional radiologic techniques in assessing acute inflammation activity, the post-operatory relapse of Crohn disease and the inflammatory component of stenosis[49], some disadvantages of this technique should be recognized. For example, the exclusive use of SPECT without CT combination cannot define anatomic changes in IBD such as stricture formation, fistula formation, or prestenotic dilation. These lesions are best demonstrated by contrast radiography[50]. Moreover, these techniques require a blood sample, followed by reinjection[41].

PET represents a relatively novel technique for monitoring IBD[50]. In contrast to the standard scintigraphy/SPECT, PET offers higher spatial and temporal resolution and is therefore more suitable for quantitative image analysis of physiological and pathologic processes[32]. However, the precise role of PET in the follow-up of paediatric patients diagnosed with IBD still remains to be defined for some clinical indication, such as differential diagnosis of fibrostenotic strictures from inflammatory strictures and as an alternative investigation after failure of conventional imaging[51].

New tracers and preclinical experiments

Radiolabelled autologous leukocytes and ^{18}F-FDG-PET represent two of the most widely adopted tracers to image IBD and other inflammatory diseases and have gained increasing acceptance for routine use. However, during the latest decade many efforts have been made in order to develop new radiopharmaceuticals able to detect inflammation and/or infection, such as labeled monoclonal antibodies, chemotactic peptides, interleukins and chemokines[52] both for SPECT and PET imaging.

SPECT tracers: Neurath *et al*[53] enrolled 59 patients with CD in a prospective study, in order to assess disease activity by FDG-PET, hydro-MRI, and immunoscintigraphy with anti-nonspecific cross-reacting antigen 95 antigranulocyte antibodies. Twelve patients with irritable bowel syndrome and 20 patients with gut cancer but without gut inflammation served as controls. All three methods

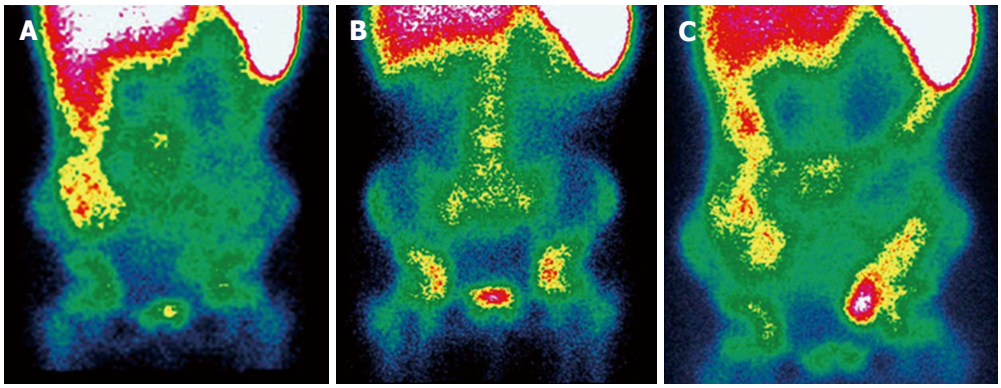

Figure 2 Three sequential ^{99m}Tc-HMPAO-white blood cell scintigraphies performed in a patient diagnosed with Crohn's disease. A: Performed at diagnosis, there is evidence of increased activity involving colon ascendens; B: Performed at follow-up after immunological therapy, a complete remission can be demonstrated; C: There is evidence of a relapse involving colon ascendens and sigma-rectum. Reprinted with permission of Springer Verlag from Caobelli *et al*[34].

showed high specificity (89%) to detect inflamed areas in the terminal ileum and colon, although analyses by hydro-MRI and granulocyte antibody scan had strikingly lower sensitivities (40.9% and 66.7%) than FDG-PET (85.4%). Although hydro-MRI showed a higher sensitivity than immunoscintigraphy, still the diagnostic performance was suboptimal. Authors concluded that FDG-PET may provide improved diagnostic accuracy compared to the other two techniques.

Annovazzi *et al*[54] compared ^{99m}Tc-HMPAO-WBC scintigraphy to ^{99m}Tc-IL2 scintigraphy in patients with CD. Both techniques provided high NPV (100% and 91%, respectively), unfortunately at expenses of a weak PPV (44% and 39%, respectively). However, only an unremarkable ^{99m}Tc-IL2 scintigraphy was associated with longer disease free survival (log-rank test, $P = 0.013$). As such, the authors hypothesized a promising role for ^{99m}Tc-IL2 scintigraphy is useful in selected patients with CD in clinical remission, who could benefit from preventive therapy to avoid disease relapse.

More recently, Van De Wiele *et al*[55] investigated three different labelling methods for monocytes (^{99m}Tc-HMPAO, ^{111}In-oxine and ^{99m}Tc-colloids for SPECT studies or ^{18}F-FDG for PET studies). Best results were yielded by ^{99m}Tc-HMPAO. *In vitro* labelled monocytes specifically accumulated in the intestinal activity foci. In 2015, Aarntzen *et al*[19] investigated the accuracy of ^{99m}Tc-CXCL8 SPECT to detect and localize disease activity in a prospective series of patients with IBD. Radiolabeled CXCL8 (IL-8) targets the CXCL8 receptors mediating chemotaxis of immune cells to the site of inflammation. The overall sensitivity and specificity on a per-patient basis for the detection of active disease was 95% and 44% for ^{99m}Tc-CXCL8 scan and 71% and 70% for endoscopy. Interestingly, the degree of ^{99m}Tc-CXCL88 accumulation correlated to the degree of neutrophilic influx in affected mucosa.

PET tracers: New more specific PET radiopharmaceuticals for inflammation of the intestinal mucosa have been investigated. A gradual shift from large proteins with a nonspecific uptake mechanism to more specific targeting proteins could be observed in the latest years.

To date, neutrophil-mediated processes, characteristic for both inflammatory and infectious processes, can be targeted in situ by radiolabeled leukocytes, antibodies or its fragments and cytokines. ^{68}Ga is one of the earliest positron-emitting radionuclides applied to clinical medicine, with a short physical half-life ($t_{1/2}$ = 68 min), allowing favorable dosimetry with consequent lower dose delivered to the patients in case of repeated imaging. This constitutes a major advantage over the SPECT agent ^{67}Ga[56].

WBC labeled with ^{18}F-FDG is a promising method for a non-invasive diagnosis and grading of intestinal inflammation. In both murine models and humans, ^{18}F-FDG-WBC PET imaging demonstrated low tracer uptake in healthy gastrointestinal and urinary tracts, where the often unpredictable glucose metabolism often hinders the specificity of ^{18}F-FDG-PET. In a study, intestinal foci of FDG-labeled WBCs were later confirmed to be inflammatory foci by histopathology. Moreover, the intensity of uptake well correlated with the degree of inflammation based on histopathologic criteria[57].

Preclinical experiments: Interleukins: Interleukins (*e.g.,* IL-1, IL-2, IL-8) have recently been proposed as potential agents for imaging infection and inflammation[52].

In a rabbit model of acute colitis, Gratz *et al*[58] investigated the diagnostic performance of ^{99m}Tc-HYNIC-IL8 scintigraphy compared to ^{99m}Tc-HMPAO-WBC scans. While both radiotracers detected colitis within 1 h after injection, ^{99m}Tc-HYNIC-IL8 images were more accurate and the absolute uptake in the affected colon continuously increased until 4 h after injection, whereas no further increase was measured for ^{99m}Tc-HMPAO-WBC beyond the first hour after the administration. The absolute uptake in the affected colon was significantly higher for ^{99m}Tc-HYNIC-IL8 than for ^{99m}Tc-HMPAO-WBC. The authors concluded that ^{99m}Tc-HYNIC-IL8 scintigraphy, unlike ^{99m}Tc-

HMPAO-WBC may provide a reliable estimation of the severity of IBD.

Preclinical experiments: (^{18}F)1-(2'-deoxy-2'-arabinofuranosyl) cytosine: The (^{18}F)1-(2'-deoxy-2'-arabinofuranosyl) cytosine (D-FAC) probe was developed as part of a broader effort to identify diverse molecular transport systems representing cellular biologic states[59].

The biodistribution of D-FAC differs from that of FDG for a higher selectivity for immune organs such as the spleen, bone marrow, and thymus. In addition, D-FAC had strikingly higher uptake in the intestine in mouse models[52]. While such increased uptake was thought to reflect the large amount of immune cells resident in the intestine mucosa, several lines of evidence revealed that intestinal D-FAC uptake is predominantly attributable to the intestinal epithelial cells. In fact, the distribution of the signal is strongly focalized in the duodenum, wherein the immune population is not significantly more expressed that in the remaining intestine[60].

Uptake of ^{18}F-D-FAC allows for a noninvasive assessment by PET. Increased uptake of D-FAC radiotracer reflects the activity of the epithelium and lymphocytes, providing a unique early marker of intestinal inflammation[59].

Preclinical experiments: (^{18}F)DPA-714: (^{18}F)DPA-714, a radioligand of a translocator protein (TSPO), is another molecular probe developed for a non-invasive quantification of the inflammatory state of IBD in animal models[61].

The TSPO is located on the outer membrane of the mitochondria and is overexpressed in the activated macrophages and microglia. This molecular event has been widely investigated in the pathologies of the central nervous system, representing a hallmark of brain inflammation. TSPO expression was recently described also in tissue samples of human colon suffering from IBD. Furthermore, its expression has been characterized in a rat model of IBD using autoradiography and immunohistochemistry[62-64].

PET imaging of IBD was conducted using ^{18}F-FDG and ^{18}F-DPA-714 in two rat models[61]. The first model was induced using dextran sodium sulfate (DSS), thus creating global inflammation in the colon, while the second one was induced by a rectal administration of trinitrobenzenesulfonic acid (TNBS), causing a local and acute inflammation.

The degree of inflammation was analyzed using PET imaging on days 7 and 8. In the first rat model, ^{18}F-DPA-714 revealed significant differences between animals treated with DSS and controls (0.50% ± 0.17% ID/cc and 0.35% ± 0.15% ID/cc, respectively). Conversely, no differences could be seen using ^{18}F-FDG. In the second model, the ^{18}F-DPA-714 uptake significantly increased from 0.46% ± 0.23% ID/cc in the controls to 1.30% ± 0.62% ID/cc in the animals treated with TNBS. As such, a correlation between PET with increased TSPO expression at cellular level was fully demonstrated. The results of this study suggest that ^{18}F-DPA-714 is suitable for studying inflammation in IBD models and could be a good molecular probe to define the degree and the localization of inflammation. Moreover, *in vivo* imaging using this TSPO ligand is potentially a powerful tool to stage and to follow inflammatory disease evolution and therapeutic efficiency at molecular level.

DISCUSSION

IBD represents a diagnostic and therapeutic challenge, not only at initial disease presentation, but also during suspected disease flares. Standard procedures like endoscopy and conventional radiologic studies are frequently required in order to assess the specific IBD subtype and evaluate disease extension and activity[34]. Although endoscopy is an essential procedure for the diagnosis and follow-up of IBD, it is invasive and able to provide only a mucosal and not transmural assessment of the colon and the distal ileal segments. Furthermore, endoscopy is not always applicable during the active phase of IBD, especially in children[48]. As such, there is the need for a noninvasive technique able to replace colonoscopy or conventional radiologic examinations in the follow-up of patients with IBD. This need is of particular importance in a paediatric population, as a highly variable response to therapy has been reported in these patients[46]. As a consequence, a technique able to assess disease activity in paediatric patients plays a major role in yielding an IBD management. Since the simple clinical remission does not well correlate with the taming of the inflammatory process at the tissue level, an effective management of IBD represents a major challenge with the currently available diagnostic modalities.

Molecular imaging presents various advantages over colonoscopy. Firstly, it is minimally invasive and well tolerated by the patients, also by paediatric ones; second, patients can undergo the procedure also during the active state of disease, without any particular limitation or precaution; third, it should be noted that no intestinal preparation is needed; fourth, molecular imaging allows the evaluation of the colon and the terminal ileum. Presence of fibrosis does not impact the results of the examination. The investigation can be repeated over time, considering an adequate time interval. This latter aspect is of relevance especially during follow-up. Finally, molecular imaging has the potential to detect and characterize the anatomic location and the disease activity at diagnosis and on therapy.

All these advantages make molecular imaging particularly suitable in paediatric patients, either when an endoscopy has been refused by the young patient or if there is any specific contraindication[34].

From the data of the literature, ^{18}F-FDG-PET, eventually fused with CT, appears to have the best potential among molecular imaging techniques, since it provides the highest accuracy both in diagnosis and follow-up. In a recent meta-analysis by Treglia *et al*[65] on 7 selected studies, including 219 patients with IBD, ^{18}F-FDG-PET

(and PET/CT) showed pooled sensitivity, specificity, positive likelihood ratio, negative likelihood ratio and diagnostic odd ratio of 85%, 87%, 6.19, 0.19 and 44.35, respectively. In their paper, the area under the ROC curve was 0.933. However, another meta-analysis by Zhang *et al*[3] including 20 prospective studies published between 1993 and 2013, did not report significant differences in sensitivity, specificity and diagnostic accuracy between ^{18}F-FDG-PET and leukocyte scintigraphy. Following their results, the authors suggested that both techniques can be alternatively used for the diagnosis of IBD, depending on their local availability. Conversely, monoclonal anti-granulocyte antibody scintigraphy showed a significantly lower sensitivity, despite the higher specificity.

During follow-up, molecular imaging proved to effectively monitor therapy response. As a matter of fact, FDG represents the whole inflammatory burden of the gut, and an early post-therapy ^{18}F-FDG-PET or PET/CT (within weeks from the start of the therapy) compared to a pre-therapy scan may allow for the early evaluation of therapy efficacy.

It seems that ^{18}F-FDG-PET or PET/CT may have different indications, depending on the subtype of IBD. Spier *et al*[25] reported that ^{18}F-FDG-PET has a good sensitivity in inflamed bowel segments in the patients with known IBD (range from 72.9% to 95.8%); while PET alone is at best suitable for patients with UC, PET/CT should be recommended in patients with CD, due to a better anatomical definition. It should also be noted that ^{18}F-FDG-PET allows the visualization of the entire bowel wall in patients with known IBD. This ability is of particular importance in patients diagnosed with CD, since this condition is often characterized by a spread to the deeper layers of the bowel wall, where endoscopy fails to detect inflammatory lesions. Furthermore, PET can assess possible overlaps between irritable bowel syndrome and IBD prior to increasing or changing immunomodulation.

Despite these advantages, the use of FDG PET/CT in a clinical setting is still indeterminate. Indeed, there is no common consensus on the timing and on the number of the post-therapy scan and the predominance of studies involving small cohorts of patients represent a limit to support the use of this imaging technique in clinical practice. Many papers in literature underlined a suboptimal specificity for ^{18}F-FDG-PET. Indeed, false positive cases due to physiologic uptake of the radiopharmaceutical in normal bowel can be often found in clinical practice. However, false positive findings can be effectively reduced with a proper distention of bowel segments through the administration of great amount of fluids[1,3,7,20,21] or by specific patients preparations as reported by Franquet *et al*[22].

In addition, a crucial question is the lack of a standardized method for quantifying accurately disease activity. Although many papers underlined the strategical role of semiquantitative parameters in PET imaging, still the huge heterogeneity of the published trials prevents to date to establish a robust assessment protocol.

It should also be mentioned that, to date, the widespread use of ^{18}F-FDG-PET/CT (and to a lesser extent of ^{99m}Tc-HMPAO-WBC scintigraphy) is hindered by relatively high costs and by relatively long waiting lists given its extensive use in oncology.

Finally, these procedures cause patient exposure to ionizing radiation (*e.g.,* about 10 mSv for ^{18}F-FDG-PET/CT, using the 50 mAs, 120 kV CT-protocol and an administered ^{18}F-FDG activity of 3.7 MBq/kg). Several studies showed that risk of cancer is greater with earlier age of exposure. Therefore it is essential to avoid unneeded ionizing radiation exposure especially in paediatrics[66]. It should be considered, however, that radiation exposure can be kept under acceptable limits by limiting the CT scan only to the abdomen-pelvis and/or using a 3D instead of a 2D scanner and a longer acquisition time with a lower administered ^{18}F-FDG activity, if patient is able to remain still, or by using new reconstruction algorithms. The replacement of CT with MRI would significantly decrease the dose of radiations and improve diagnostic information on structural changes in bowel wall, despite a longer duration of the examination[1,2,4-7,21,67]. Finally, considering an adequate time interval between serial examinations would limit the radioexposure into acceptable limits.

In conclusion, WBC scintigraphy and ^{18}F-FDG-PET (alone or combined with CT or, in a next future, with MRI) represent a useful tool to detect active disease in IBD. However, the available data need to be validated in prospective multicenter studies on larger patient samples. Furthermore, even better diagnostic performance may be envisioned thanks to more specific and accurate radiotracers, which are however to date still far from a clinical validation in the clinical setting.

COMMENTS

Background

Inflammatory bowel disease (IBD) is a chronic inflammatory condition, in which the integrity of the gut epithelium represents a major pathophysiological step. Although endoscopy and barium radiological examinations are the diagnostic "gold standard" for IBD, both techniques require a specific patient preparation, not always feasible or easily tolerated.

Research frontiers

Molecular imaging with single photon emission tomography (SPECT) and positron emission tomography (PET) may be a reliable, non-invasive, accurate and easily reproducible diagnostic tool, able to assess location, extent and activity grade of IBD.

Innovations and breakthroughs

The present Review is to date the most comprehensive, including all imaging modalities (*i.e.,* SPECT, SPECT/CT, PET, PET/CT) and various radiopharmaceuticals. Moreover, interesting data about experimental procedures are provided.

Applications

The present Review aims at becoming a useful guide for the Clinicians who may want to plan an effective diagnostic assessment in patients with IBD. Furthermore, the knowledge of the state-of-the-art of molecular imaging provides a useful tool

able to monitor the effectiveness of the therapy.

Terminology

SPECT: Single photon emission tomography. This technique is based on the administration of gamma-emitting radiopharmaceuticals, following the normal metabolic pathways. The uptake is detected by means of gamma-cameras, able to localize possible foci of increased uptakes, consistent with inflammation and/or infection. PET: Positron emission tomography. This technique is based on the administration of positron emitting radiopharmaceuticals, also following the normal metabolic pathways. The uptake is detected by means of PET scanners, whose spatial and temporal resolution is significantly higher than those of SPECT cameras.

Peer-review

This is an extensive review on nuclear medicine investigations in IBD, for diagnosis and follow-up. The authors nicely reported also in tables the large existing literature.

REFERENCES

1 **Das CJ**, Makharia GK, Kumar R, Kumar R, Tiwari RP, Sharma R, Malhotra A. PET/CT colonography: a novel non-invasive technique for assessment of extent and activity of ulcerative colitis. *Eur J Nucl Med Mol Imaging* 2010; **37**: 714-721 [PMID: 20033154 DOI: 10.1007/s00259-009-1335-2]

2 **Holtmann MH**, Uenzen M, Helisch A, Dahmen A, Mudter J, Goetz M, Schreckenberger M, Galle PR, Bartenstein P, Neurath MF. 18F-Fluorodeoxyglucose positron-emission tomography (PET) can be used to assess inflammation non-invasively in Crohn's disease. *Dig Dis Sci* 2012; **57**: 2658-2668 [PMID: 22569824 DOI: 10.1007/s10620-012-2190-8]

3 **Zhang J**, Li LF, Zhu YJ, Qiu H, Xu Q, Yang J, Weng WW, Liu NH. Diagnostic performance of 18F-FDG-PET versus scintigraphy in patients with inflammatory bowel disease: a meta-analysis of prospective literature. *Nucl Med Commun* 2014; **35**: 1233-1246 [PMID: 25192191 DOI: 10.1097/MNM.0000000000000202]

4 **Lenze F**, Wessling J, Bremer J, Ullerich H, Spieker T, Weckesser M, Gonschorrek S, Kannengiesser K, Rijcken E, Heidemann J, Luegering A, Schober O, Domschke W, Kucharzik T, Maaser C. Detection and differentiation of inflammatory versus fibromatous Crohn's disease strictures: prospective comparison of 18F-FDG-PET/CT, MR-enteroclysis, and transabdominal ultrasound versus endoscopic/histologic evaluation. *Inflamm Bowel Dis* 2012; **18**: 2252-2260 [PMID: 22359277 DOI: 10.1002/ibd.22930]

5 **Catalano OA**, Gee MS, Nicolai E, Selvaggi F, Pellino G, Cuocolo A, Luongo A, Catalano M, Rosen BR, Gervais D, Vangel MG, Soricelli A, Salvatore M. Evaluation of Quantitative PET/MR Enterography Biomarkers for Discrimination of Inflammatory Strictures from Fibrotic Strictures in Crohn Disease. *Radiology* 2016; **278**: 792-800 [PMID: 26436860 DOI: 10.1148/radiol.2015150566]

6 **Meisner RS**, Spier BJ, Einarsson S, Roberson EN, Perlman SB, Bianco JA, Taylor AJ, Einstein M, Jaskowiak CJ, Massoth KM, Reichelderfer M. Pilot study using PET/CT as a novel, noninvasive assessment of disease activity in inflammatory bowel disease. *Inflamm Bowel Dis* 2007; **13**: 993-1000 [PMID: 17394243 DOI: 10.1002/ibd.20134]

7 **Ahmadi A**, Li Q, Muller K, Collins D, Valentine JF, Drane W, Polyak S. Diagnostic value of noninvasive combined fluorine-18 labeled fluoro-2-deoxy-D-glucose positron emission tomography and computed tomography enterography in active Crohn's disease. *Inflamm Bowel Dis* 2010; **16**: 974-981 [PMID: 19885907 DOI: 10.1002/ibd.21153]

8 **Lachter J**, Isseroff HN, Yasin K, Keidar Z, Israel O. Radiolabeled leukocyte imaging in inflammatory bowel disease: a prospective blinded evaluation. *Hepatogastroenterology* 2003; **50**: 1439-1441 [PMID: 14571757]

9 **Paredes JM**, Ripollés T, Cortés X, Reyes MD, López A, Martínez MJ, Moreno-Osset E. Non-invasive diagnosis and grading of postsurgical endoscopic recurrence in Crohn's disease: usefulness of abdominal ultrasonography and (99m)Tc-hexamethylpropylene amineoxime-labelled leucocyte scintigraphy. *J Crohns Colitis* 2010; **4**: 537-545 [PMID: 21122557 DOI: 10.1016/j.crohns.2010.03.002]

10 **Kerry JE**, Marshall C, Griffiths PA, James MW, Scott BB. Comparison between Tc-HMPAO labelled white cells and Tc LeukoScan in the investigation of inflammatory bowel disease. *Nucl Med Commun* 2005; **26**: 245-251 [PMID: 15722905]

11 **Biancone L**, Schillaci O, Capoccetti F, Bozzi RM, Fina D, Petruzziello C, Geremia A, Simonetti G, Pallone F. Technetium-99m-HMPAO labeled leukocyte single photon emission computerized tomography (SPECT) for assessing Crohn's disease extent and intestinal infiltration. *Am J Gastroenterol* 2005; **100**: 344-354 [PMID: 15667492 DOI: 10.1111/j.1572-0241.2005.41123.x]

12 **Hillel PG**, Lorenz E, Metherall P, Tindale WB. 99mTc white-cell imaging in inflammatory bowel disease: a comparison of planar versus SPECT. *Nucl Med Commun* 2011; **32**: 591-596 [PMID: 21423061 DOI: 10.1097/MNM.0b013e328345b2fd]

13 **Mota LG**, Coelho LG, Simal CJ, Ferrari ML, Toledo C, Martin-Comin J, Diniz SO, Cardoso VN. Leukocyte-technetium-99m uptake in Crohn's disease: does it show subclinical disease? *World J Gastroenterol* 2010; **16**: 365-371 [PMID: 20082484 DOI: 10.3748/WJG.v16.i3.365]

14 **Rowe FA**, Camilleri M, Forstrom LA, Batts KP, Mullan BP, Thomforde GM, Dunn W, Zinsmeister AR. A pilot study of splenic and whole body retention of autologous radiolabeled leukocytes in the assessment of severity in inflammatory colitis. *Am J Gastroenterol* 1995; **90**: 1771-1775 [PMID: 7572892]

15 **Cheow HK**, Voutnis DD, Evans JW, Szczepura KR, Swift EA, Bird NJ, Ruparelia P, Solanki CK, Ballinger JR, Chilvers ER, Middleton SJ, Peters AM. Quantification of disease activity in patients undergoing leucocyte scintigraphy for suspected inflammatory bowel disease. *Eur J Nucl Med Mol Imaging* 2005; **32**: 329-337 [PMID: 15791443 DOI: 10.1007/s00259-004-1617-7]

16 **Van den Brande JM**, Koehler TC, Zelinkova Z, Bennink RJ, te Velde AA, ten Cate FJ, van Deventer SJ, Peppelenbosch MP, Hommes DW. Prediction of antitumour necrosis factor clinical efficacy by real-time visualisation of apoptosis in patients with Crohn's disease. *Gut* 2007; **56**: 509-517 [PMID: 17082252 DOI: 10.1136/gut.2006.105379]

17 **Bicik I**, Bauerfeind P, Breitbach T, von Schulthess GK, Fried M. Inflammatory bowel disease activity measured by positron-emission tomography. *Lancet* 1997; **350**: 262 [PMID: 9242806 DOI: 10.1016/S0140-6736(05)62225-8]

18 **Skehan SJ**, Issenman R, Mernagh J, Nahmias C, Jacobson K. 18F-fluorodeoxyglucose positron tomography in diagnosis of paediatric inflammatory bowel disease. *Lancet* 1999; **354**: 836-837 [PMID: 10485733 DOI: 10.1016/S0140-6736(99)80021-X]

19 **Aarntzen EH**, Hermsen R, Drenth JP, Boerman OC, Oyen WJ. 99mTc-CXCL8 SPECT to Monitor Disease Activity in Inflammatory Bowel Disease. *J Nucl Med* 2016; **57**: 398-403 [PMID: 26609182 DOI: 10.2967/jnumed.115.165795]

20 **Groshar D**, Bernstine H, Stern D, Sosna J, Eligalashvili M, Gurbuz EG, Niv Y, Fraser G. PET/CT enterography in Crohn disease: correlation of disease activity on CT enterography with 18F-FDG uptake. *J Nucl Med* 2010; **51**: 1009-1014 [PMID: 20554741 DOI: 10.2967/jnumed.109.073130]

21 **Shyn PB**, Mortele KJ, Britz-Cunningham SH, Friedman S, Odze RD, Burakoff R, Goldberg JE, Erturk M, Silverman SG. Low-dose 18F-FDG PET/CT enterography: improving on CT enterography assessment of patients with Crohn disease. *J Nucl Med* 2010; **51**: 1841-1848 [PMID: 21078803 DOI: 10.2967/jnumed.110.080796]

22 **Franquet E**, Palmer MR, Gifford AE, Selen DJ, Chen YC, Sedora-Roman N, Joyce RM, Kolodny GM, Moss AC. Rifaximin suppresses background intestinal 18F-FDG uptake on PET/CT scans. *Nucl Med Commun* 2014; **35**: 1026-1031 [PMID: 25076161 DOI: 10.1097/MNM.0000000000000170]

23 **Louis E**, Ancion G, Colard A, Spote V, Belaiche J, Hustinx R. Noninvasive assessment of Crohn's disease intestinal lesions with (18)F-FDG PET/CT. *J Nucl Med* 2007; **48**: 1053-1059 [PMID: 17574978 DOI: 10.2967/jnumed.107.040436]

24 **Das CJ**, Makharia G, Kumar R, Chawla M, Goswami P, Sharma R, Malhotra A. PET-CT enteroclysis: a new technique for evaluation of inflammatory diseases of the intestine. *Eur J Nucl Med Mol Imaging* 2007; **34**: 2106-2114 [PMID: 17710395 DOI: 10.1007/s00259-007-0525-z]

25 **Spier BJ**, Perlman SB, Jaskowiak CJ, Reichelderfer M. PET/CT in the evaluation of inflammatory bowel disease: studies in patients before and after treatment. *Mol Imaging Biol* 2010; **12**: 85-88 [PMID: 19430844 DOI: 10.1007/s11307-009-0232-1]

26 **Glaudemans AW**, de Vries EF, Galli F, Dierckx RA, Slart RH, Signore A. The use of (18)F-FDG-PET/CT for diagnosis and treatment monitoring of inflammatory and infectious diseases. *Clin Dev Immunol* 2013; **2013**: 623036 [PMID: 24027590 DOI: 10.1155/2013/623036]

27 **Rubin DT**, Surma BL, Gavzy SJ, Schnell KM, Bunnag AP, Huo D, Appelbaum DE. Positron emission tomography (PET) used to image subclinical inflammation associated with ulcerative colitis (UC) in remission. *Inflamm Bowel Dis* 2009; **15**: 750-755 [PMID: 19090558 DOI: 10.1002/ibd.20819]

28 **Lapp RT**, Spier BJ, Perlman SB, Jaskowiak CJ, Reichelderfer M. Clinical utility of positron emission tomography/computed tomography in inflammatory bowel disease. *Mol Imaging Biol* 2011; **13**: 573-576 [PMID: 20574849 DOI: 10.1007/s11307-010-0367-0]

29 **Jacene HA**, Ginsburg P, Kwon J, Nguyen GC, Montgomery EA, Bayless TM, Wahl RL. Prediction of the need for surgical intervention in obstructive Crohn's disease by 18F-FDG PET/CT. *J Nucl Med* 2009; **50**: 1751-1759 [PMID: 19837758 DOI: 10.2967/jnumed.109.065466]

30 **Kuwaki K**, Mitsuyama K, Kaida H, Takedatsu H, Yoshioka S, Yamasaki H, Yamauchi R, Fukunaga S, Abe T, Tsuruta O, Torimura T. A longitudinal study of FDG-PET in Crohn disease patients receiving granulocyte/monocyte apheresis therapy. *Cytotherapy* 2016; **18**: 291-299 [PMID: 26700210 DOI: 10.1016/j.jcyt.2015.10.010]

31 **Saboury B**, Salavati A, Brothers A, Basu S, Kwee TC, Lam MG, Hustinx R, Louis E, Torigian DA, Alavi A. FDG PET/CT in Crohn's disease: correlation of quantitative FDG PET/CT parameters with clinical and endoscopic surrogate markers of disease activity. *Eur J Nucl Med Mol Imaging* 2014; **41**: 605-614 [PMID: 24253895 DOI: 10.1007/s00259-013-2625-2]

32 **Alberini JL**, Badran A, Freneaux E, Hadji S, Kalifa G, Devaux JY, Dupont T. Technetium-99m HMPAO-labeled leukocyte imaging compared with endoscopy, ultrasonography, and contrast radiology in children with inflammatory bowel disease. *J Pediatr Gastroenterol Nutr* 2001; **32**: 278-286 [PMID: 11345176]

33 **Charron M**, del Rosario FJ, Kocoshis SA. Pediatric inflammatory bowel disease: assessment with scintigraphy with 99mTc white blood cells. *Radiology* 1999; **212**: 507-513 [PMID: 10429710 DOI: 10.1148/radiology.212.2.r99au45507]

34 **Caobelli F**, Panarotto MB, Andreoli F, Ravelli A, De Agostini A, Giubbini R. Is 99mTc-HMPAO granulocyte scan an alternative to endoscopy in pediatric chronic inflammatory bowel disease (IBD)? *Eur J Pediatr* 2011; **170**: 51-57 [PMID: 20669028 DOI: 10.1007/s00431-010-1269-5]

35 **Cucchiara S**, Celentano L, de Magistris TM, Montisci A, Iula VD, Fecarotta S. Colonoscopy and technetium-99m white cell scan in children with suspected inflammatory bowel disease. *J Pediatr* 1999; **135**: 727-732 [PMID: 10586176]

36 **Charron M**, del Rosario JF, Kocoshis S. Use of technetium-tagged white blood cells in patients with Crohn's disease and ulcerative colitis: is differential diagnosis possible? *Pediatr Radiol* 1998; **28**: 871-877 [PMID: 9799322 DOI: 10.1007/s002470050486]

37 **Charron M**, Di Lorenzo C, Kocoshis S. Are 99mTc leukocyte scintigraphy and SBFT studies useful in children suspected of having inflammatory bowel disease? *Am J Gastroenterol* 2000; **95**: 1208-1212 [PMID: 10811329 DOI: 10.1111/j.1572-0241.2000.02011.x]

38 **Davison SM**, Chapman S, Murphy MS. 99mTc-HMPAO leucocyte scintigraphy fails to detect Crohn's disease in the proximal gastrointestinal tract. *Arch Dis Child* 2001; **85**: 43-46 [PMID: 11420197]

39 **Grahnquist L**, Chapman SC, Hvidsten S, Murphy MS. Evaluation of 99mTc-HMPAO leukocyte scintigraphy in the investigation of pediatric inflammatory bowel disease. *J Pediatr* 2003; **143**: 48-53 [PMID: 12915823 DOI: 10.1016/S0022-3476(03)00280-4]

40 **Peacock K**, Porn U, Howman-Giles R, O'Loughlin E, Uren R, Gaskin K, Dorney S, Kamath R. 99mTc-stannous colloid white cell scintigraphy in childhood inflammatory bowel disease. *J Nucl Med* 2004; **45**: 261-265 [PMID: 14960645]

41 **Bruno I**, Martelossi S, Geatti O, Maggiore G, Guastalla P, Povolato M, Ventura A. Antigranulocyte monoclonal antibody immunoscintigraphy in inflammatory bowel disease in children and young adolescents. *Acta Paediatr* 2002; **91**: 1050-1055 [PMID: 12434889]

42 **Lemberg DA**, Issenman RM, Cawdron R, Green T, Mernagh J, Skehan SJ, Nahmias C, Jacobson K. Positron emission tomography in the investigation of pediatric inflammatory bowel disease. *Inflamm Bowel Dis* 2005; **11**: 733-738 [PMID: 16043988 DOI: 10.1097/01.MIB.0000172810.49619.cb]

43 **Löffler M**, Weckesser M, Franzius C, Schober O, Zimmer KP. High diagnostic value of 18F-FDG-PET in pediatric patients with chronic inflammatory bowel disease. *Ann N Y Acad Sci* 2006; **1072**: 379-385 [PMID: 17057218 DOI: 10.1196/annals.1326.014]

44 **Däbritz J**, Jasper N, Loeffler M, Weckesser M, Foell D. Noninvasive assessment of pediatric inflammatory bowel disease with ^{18}F-fluorodeoxyglucose-positron emission tomography and computed tomography. *Eur J Gastroenterol Hepatol* 2011; **23**: 81-89 [PMID: 21042220 DOI: 10.1097/MEG.0b013e3283410222]

45 **Berthold LD**, Steiner D, Scholz D, Alzen G, Zimmer KP. Imaging of chronic inflammatory bowel disease with 18F-FDG PET in children and adolescents. *Klin Padiatr* 2013; **225**: 212-217 [PMID: 23519750 DOI: 10.1055/s-0033-1334878]

46 **Giaffer MH**, Tindale WB, Holdsworth D. Value of technetium-99m HMPAO-labelled leucocyte scintigraphy as an initial screening test in patients suspected of having inflammatory bowel disease. *Eur J Gastroenterol Hepatol* 1996; **8**: 1195-1200 [PMID: 8980940]

47 **Chroustova D**, Volf V, Kleisner I, Doubravska M. 99mTc-HMPAO-Labelled Leukocytes Scintigraphy in Monitoring Children and Adolescents with IBD. *Current Radiopharma* 2009; **2:** 18-23

48 **Papós M**, Várkonyi A, Láng J, Buga K, Tímár E, Polgár M, Bódi I, Csernay L. HM-PAO-labeled leukocyte scintigraphy in pediatric patients with inflammatory bowel disease. *J Pediatr Gastroenterol Nutr* 1996; **23**: 547-552 [PMID: 8985843]

49 **Verdú Rico J**, Juste Ruiz M, Jover R, Muñoz Acosta J, Muñoz J, Martínez Caballero A, Antón Leal A, Caballero Carpena O. [99mTc-HMPAO-leukocyte-labeled scintigraphy in the detection and follow-up of inflammatory bowel disease]. *An Pediatr* (Barc) 2006; **64**: 457-463 [PMID: 16756887]

50 **Del Rosario MA**, Fitzgerald JF, Siddiqui AR, Chong SK, Croffie JM, Gupta SK. Clinical applications of technetium Tc 99m hexamethyl propylene amine oxime leukocyte scan in children with inflammatory bowel disease. *J Pediatr Gastroenterol Nutr* 1999; **28**: 63-70 [PMID: 9890471 DOI: 10.1097/00005176-199901000-00015]

51 **Halpenny DF**, Burke JP, Lawlor GO, O'Connell M. Role of PET and combination PET/CT in the evaluation of patients with inflammatory bowel disease. *Inflamm Bowel Dis* 2009; **15**: 951-958 [PMID: 19130618 DOI: 10.1002/ibd.20817]

52 **Basu S**, Zhuang H, Torigian DA, Rosenbaum J, Chen W, Alavi A. Functional imaging of inflammatory diseases using nuclear medicine techniques. *Semin Nucl Med* 2009; **39**: 124-145 [PMID: 19187805 DOI: 10.1053/j.semnuclmed.2008.10.006]

53 **Neurath MF**, Vehling D, Schunk K, Holtmann M, Brockmann H, Helisch A, Orth T, Schreckenberger M, Galle PR, Bartenstein P. Noninvasive assessment of Crohn's disease activity: a comparison of 18F-fluorodeoxyglucose positron emission tomography, hydromagnetic resonance imaging, and granulocyte scintigraphy with labeled antibodies. *Am J Gastroenterol* 2002; **97**: 1978-1985 [PMID: 12190164 DOI: 10.1111/j.1572-0241.2002.05836.x]

54 **Annovazzi A**, Biancone L, Caviglia R, Chianelli M, Capriotti G, Mather SJ, Caprilli R, Pallone F, Scopinaro F, Signore A. 99mTc-

interleukin-2 and (99m)Tc-HMPAO granulocyte scintigraphy in patients with inactive Crohn's disease. *Eur J Nucl Med Mol Imaging* 2003; **30**: 374-382 [PMID: 12634965 DOI: 10.1007/s00259-002-1069-x]

55 **Van De Wiele C**, Sathekge M, Maes A. Targeting monocytes and macrophages by means of SPECT and PET. *Q J Nucl Med Mol Imaging* 2014; **58**: 269-275 [PMID: 24844256]

56 **Silvola JM**, Laitinen I, Sipilä HJ, Laine VJ, Leppänen P, Ylä-Herttuala S, Knuuti J, Roivainen A. Uptake of 68gallium in atherosclerotic plaques in LDLR-/-ApoB100/100 mice. *EJNMMI Res* 2011; **1**: 14 [PMID: 22214258 DOI: 10.1186/2191-219X-1-14]

57 **Pio BS**, Byrne FR, Aranda R, Boulay G, Spicher K, Song MH, Birnbaumer L, Phelps ME, Czernin J, Silverman DH. Noninvasive quantification of bowel inflammation through positron emission tomography imaging of 2-deoxy-2-[18F]fluoro-D-glucose-labeled white blood cells. *Mol Imaging Biol* 2003; **5**: 271-277 [PMID: 14499142]

58 **Gratz S**, Rennen HJ, Boerman OC, Oyen WJ, Corstens FH. Rapid imaging of experimental colitis with (99m)Tc-interleukin-8 in rabbits. *J Nucl Med* 2001; **42**: 917-923 [PMID: 11390557]

59 **Brewer S**, Nair-Gill E, Wei B, Chen L, Li X, Riedinger M, Campbell DO, Wiltzius S, Satyamurthy N, Phelps ME, Radu C, Witte ON, Braun J. Epithelial uptake of [18F]1-(2'-deoxy-2'-arabinofuranosyl) cytosine indicates intestinal inflammation in mice. *Gastroenterology* 2010; **138**: 1266-1275 [PMID: 20080095 DOI: 10.1053/j.gastro.2010.01.003]

60 **Blumenthal RD**, Sharkey RM, Kashi R, Natale AM, Goldenberg DM. Physiological factors influencing radioantibody uptake: a study of four human colonic carcinomas. *Int J Cancer* 1992; **51**: 935-941 [PMID: 1322378]

61 **Bernards N**, Pottier G, Thézé B, Dollé F, Boisgard R. In vivo evaluation of inflammatory bowel disease with the aid of μPET and the translocator protein 18 kDa radioligand [18F]DPA-714. *Mol Imaging Biol* 2015; **17**: 67-75 [PMID: 25015387 DOI: 10.1007/s11307-014-0765-9]

62 **Martín A**, Boisgard R, Thézé B, Van Camp N, Kuhnast B, Damont A, Kassiou M, Dollé F, Tavitian B. Evaluation of the PBR/TSPO radioligand [(18)F]DPA-714 in a rat model of focal cerebral ischemia. *J Cereb Blood Flow Metab* 2010; **30**: 230-241 [PMID: 19794397 DOI: 10.1038/jcbfm.2009.205]

63 **Abourbeh G**, Thézé B, Maroy R, Dubois A, Brulon V, Fontyn Y, Dollé F, Tavitian B, Boisgard R. Imaging microglial/macrophage activation in spinal cords of experimental autoimmune encephalomyelitis rats by positron emission tomography using the mitochondrial 18 kDa translocator protein radioligand [^{18}F]DPA-714. *J Neurosci* 2012; **32**: 5728-5736 [PMID: 22539835 DOI: 10.1523/JNEUROSCI.2900-11.2012]

64 **Ostuni MA**, Issop L, Péranzi G, Walker F, Fasseu M, Elbim C, Papadopoulos V, Lacapere JJ. Overexpression of translocator protein in inflammatory bowel disease: potential diagnostic and treatment value. *Inflamm Bowel Dis* 2010; **16**: 1476-1487 [PMID: 20222126 DOI: 10.1002/ibd.21250]

65 **Treglia G**, Quartuccio N, Sadeghi R, Farchione A, Caldarella C, Bertagna F, Fania P, Cistaro A. Diagnostic performance of Fluorine-18-Fluorodeoxyglucose positron emission tomography in patients with chronic inflammatory bowel disease: a systematic review and a meta-analysis. *J Crohns Colitis* 2013; **7**: 345-354 [PMID: 22960135 DOI: 10.1016/j.crohns.2012.08.005]

66 **Sauer CG**. Radiation exposure in children with inflammatory bowel disease. *Curr Opin Pediatr* 2012; **24**: 621-626 [PMID: 22935753 DOI: 10.1097/MOP.0b013e32835742a2]

67 **Perlman SB**, Hall BS, Reichelderfer M. PET/CT imaging of inflammatory bowel disease. *Semin Nucl Med* 2013; **43**: 420-426 [PMID: 24094709 DOI: 10.1053/j.semnuclmed.2013.06.006]

P- Reviewer: Annese V, Capasso R, Fries W, Giron MC
S- Editor: Qi Y **L- Editor**: A **E- Editor**: Li D

World Journal of Radiology

Submit a Manuscript: http://www.wjgnet.com/esps/
Help Desk: http://www.wjgnet.com/esps/helpdesk.aspx
DOI: 10.4329/wjr.v8.i10.846

World J Radiol 2016 October 28; 8(10): 846-850
ISSN 1949-8470 (online)

CASE REPORT

Presumptive case of sparganosis manifesting as a hepatic mass: A case report and literature review

Gyeong Deok Jo, Jae Young Lee, Sung-Tae Hong, Jung Hoon Kim, Joon Koo Han

Gyeong Deok Jo, Department of Medicine, Seoul National University School of Medicine, Jongno-gu, Seoul 03080, South Korea

Jae Young Lee, Jung Hoon Kim, Joon Koo Han, Department of Radiology, Seoul National University Hospital, Jongno-gu, Seoul 03080, South Korea

Jae Young Lee, Jung Hoon Kim, Joon Koo Han, Institute of Radiation Medicine, Seoul National University Hospital, Jongno-gu, Seoul 03080, South Korea

Sung-Tae Hong, Department of Parasitology and Tropical Medicine, Seoul National University College of Medicine, Jongno-gu, Seoul 03080, South Korea

Sung-Tae Hong, Institute of Endemic Diseases, Seoul National University College of Medicine, Jongno-gu, Seoul 03080, South Korea

Author contributions: Jo GD and Lee JY designed the research and wrote the paper; Hong ST, Kim JH and Han JK analyzed and interpreted results.

Institutional review board statement: The study was reviewed and approved by the Seoul National University Hospital Institutional Review Board.

Informed consent statement: We were given exemption from getting informed consent by the Institutional Review Board.

Conflict-of-interest statement: The authors declare that they have no conflict of interest.

Manuscript source: Unsolicited manuscript

Correspondence to: Jae Young Lee, MD, PhD, Department of Radiology, Seoul National University Hospital, 101 Daehak-ro, Jongno-gu, Seoul 03080, South Korea. leejy4u@snu.ac.kr
Telephone: +82-2-20723107
Fax: +82-2-7436385

Received: March 7, 2016
Peer-review started: March 9, 2016
First decision: May 19, 2016
Revised: July 26, 2016
Accepted: August 17, 2016
Article in press: August 18, 2016
Published online: October 28, 2016

Abstract

A 60-year-old man was admitted due to rectosigmoid colon cancer, and a hepatic mass was incidentally found during the staging work-up. The mass appeared cystic with a thick wall and contained multiple bizarre cord-like structures on ultrasound, computed tomography and magnetic resonance imaging. The differential diagnoses included organizing abscess/hematoma, foreign body granuloma and parasite infestation. Serologic study revealed anti-sparganum antibodies. Over 4-year follow-up, the patient did not complain of symptoms, and no changes in the characteristics of the liver mass were observed. Hepatic sparganosis is rare; only two cases have been clinically reported, and no detailed radiologic description was available until now. This case report presents a detailed radiologic description of a hepatic mass that could most likely represent hepatic sparganosis.

Key words: Ultrasonography; Parasites; Sparganosis; Magnetic resonance imaging; Computed tomography; Liver

Core tip: Hepatic sparganosis is rare; only two cases have been clinically reported, and no detailed radiologic description was available until now. This report presents radiologic findings of a presumptive case of sparganosis manifesting as a hepatic mass. This hepatic mass showed nonenhancing low attenuation mass with bizarrely arranged calcified internal cord-like structures on computed tomography, a necrotic mass with internal serpiginous tubular structures on magnetic resonance imaging, and a well-defined mixed echoic mass with multiple cord-like structures on ultrasonography. The understanding of this case will help physicians to consider the possibility of hepatic sparganosis when they encounter hepatic masses with bizarrely arranged internal serpiginous structures.

Jo GD, Lee JY, Hong ST, Kim JH, Han JK. Presumptive case of sparganosis manifesting as a hepatic mass: A case report and literature review. *World J Radiol* 2016; 8(10): 846-850 Available from: URL: http://www.wjgnet.com/1949-8470/full/v8/i10/846.htm DOI: http://dx.doi.org/10.4329/wjr.v8.i10.846

INTRODUCTION

Sparganosis refers to a parasitic infestation of plerocercoid larva of *Spirometra*. Humans can serve as second intermediate hosts, paratenic hosts and occasionally definitive hosts. Three routes of infection are currently known. The first is the direct ingestion of live plerocercoid larva *via* the consumption of raw second intermediate hosts (amphibians, reptiles, avians, mammals, *etc*.). The second is the consumption of water containing *Cyclops* species infected with procercoid larva. The third method route of infection is the use of the flesh or skin of infected frogs or snakes as a poultice. Regions of high prevalence are located in Asian countries, including China, Japan, Thailand and South Korea[1]. Sparganosis frequently involves the abdominal wall, scrotum, lower extremities and thoracic wall. Less frequently involved areas include the abdominal cavity, pleural cavity, vertebral canal and orbit[2]. Regarding the liver, only two cases of sparganosis have previously been reported to the best of our knowledge. Khurana *et al*[3] reported a case of hepatic sparganosis in the English literature in 2012. The other case of hepatic sparganosis was reported in 1990 in the Korean literature[4]. Unfortunately, neither of these case reports contain sufficient radiologic findings of hepatic sparganosis because they did not contain radiologic images or descriptions of computed tomography (CT) or magnetic resonance (MR) imaging findings but only included ultrasonography (US) findings.

CASE REPORT

A 60-year-old man with rectosigmoid colon cancer was referred to our hospital for preoperative staging evaluation. He was diagnosed with rectosigmoid colon cancer at a regular health checkup. During an abdominal CT study performed for the staging of the rectosigmoid colon cancer, a large low-attenuation mass was incidentally detected in the liver. This mass had internal bizarrely arranged cord-like structures, calcifications, and a few focal areas of fat (Figure 1). Our primary radiologic impression was a teratoma. Angiomyolipoma and myxoid liposarcoma were included in the differential diagnosis. Cystic metastasis of colon cancer was described as the least likely differential diagnosis.

For further evaluation, gadolinium-enhanced liver MR imaging was performed (Figure 2). Serpiginous tubular structures were clearly observed on T2-weighted images (Figure 2B). Diffusion in the mass was not restricted (Figure 2C and D). Axial in-phase T1-weighted and opposed-phase T1-weighted images showed multiple small foci with signal drops in opposed-phase image that are indicative of the presence of microscopic fat deposits. These findings indicated a fat-containing totally necrotic mass or a cystic mass with internal dead tissue. Our differential diagnosis included an organizing abscess/hematoma, a foreign body granuloma, and parasite infestation. Colon cancer metastasis was considered unlikely.

Liver US was performed to further evaluate the internal content of the liver mass. The mass was well demarcated upon US and contained echogenic material and serpiginous echogenic structures with a low echoic tubular rim (Figure 3). No vascularity was observed in the mass on color Doppler US. These findings led us to place foreign body granuloma and parasite-induced granuloma at the top of the list of differentials.

In a complete blood count including a differential cell count, no leukocytosis (white blood cell 5.02 × $10^3/\mu L$) was observed, and the proportion of eosinophils was normal (2%). Because decreased liver excretory function was found on an indocyanine green excretion test, only an anterior resection of the rectosigmoid colon cancer without liver resection was conducted. The patient was discharged and followed up on an outpatient basis.

ELISA was performed two months after surgery to identify the parasite. The patient's serum was tested for antibodies against *Clonorchis*, *Paragonimus*, *Cysticercus* and *Sparganum*. Only anti-sparganum antibodies were detected at a titer that was 1.4-fold of the cutoff value (positive and negative control sera were used to rule out the possibility of false negativity and false positivity). Although the treatment of choice for sparganosis is surgical removal, this approach was not employed due to the decreased liver excretory function. The hepatic mass was left untreated and regularly followed up.

The patient denied eating raw or undercooked snake or frog flesh and applying the skin or flesh of these animals to a wound as a poultice but admitted to drinking mountain water several times. Because he had a history of travel to the middle East for two years, which is a crucial diagnostic clue for echinococcosis[5], and serpiginous linear structures could also be observed in echinococcal cysts[6], an additional ELISA test was

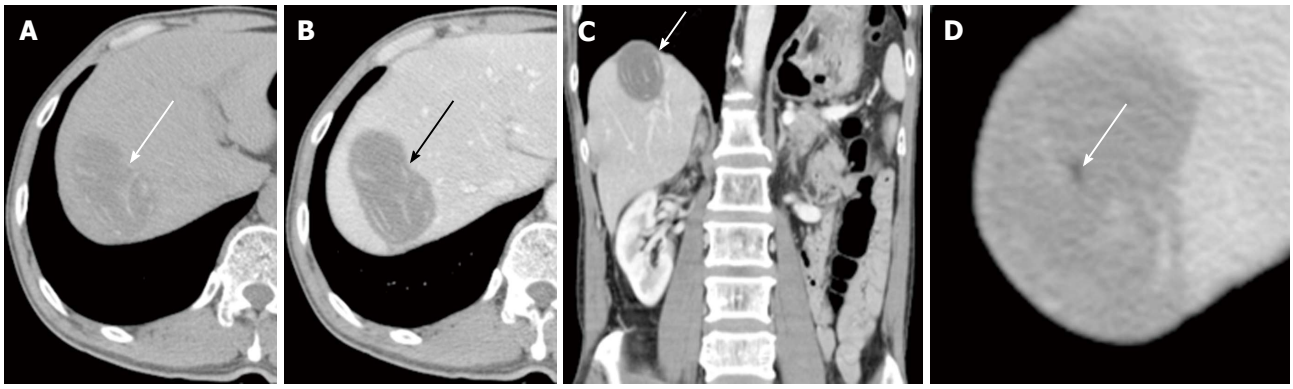

Figure 1 Liver computed tomography imaging. A: Axial noncontrast computed tomography (CT) image showing an ovoid low attenuation lesion (arrow) in the right hepatic dome. This mass has internal linear or curvilinear cord-like lesions that are most likely calcified. This mass (arrow) measured 6.3 cm × 3.5 cm. B: Axial contrast-enhanced CT image clearly showing that this ovoid lesion (arrow) does not have any enhanced portions, which suggests a totally necrotic lesion or a cystic mass. The internal cord-like structures are bizarrely arranged; C: Coronal contrast-enhanced CT image showing that the internal structures within the mass (arrow) are arranged in a whirling manner; D: Low attenuation (-22 Hounsfield units) region (arrow) in the center of the mass on a contrast-enhanced CT image, suggesting the presence of a small amount of fat.

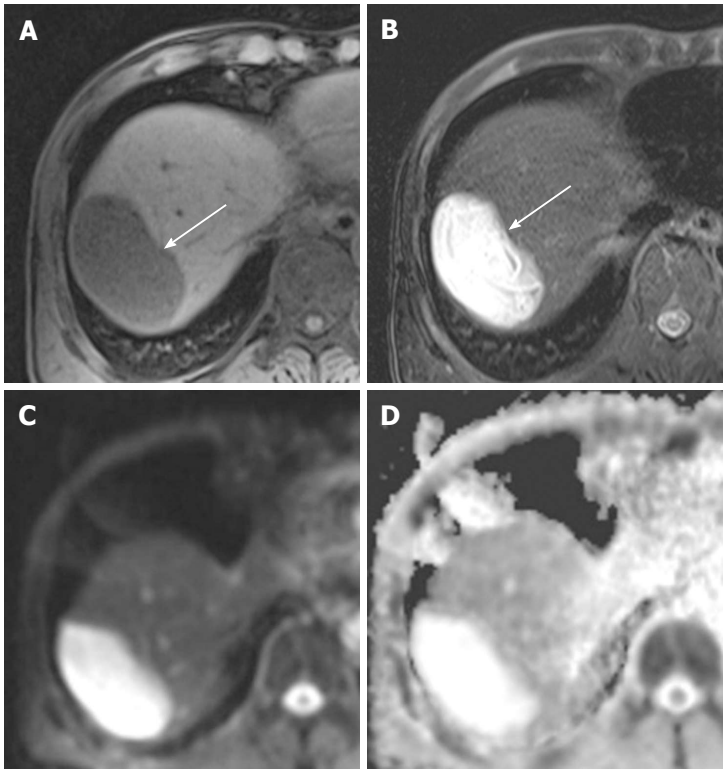

Figure 2 Liver magnetic resonance imaging. A: Axial nonenhanced T1-weighted image showing that this hepatic mass (arrow) exhibits homogeneously low signal intensity; B: Fat-saturated axial T2-weighted image showing that the mass (arrow) exhibits very high signal intensity and internal serpiginous tubular structures; C and D: Axial diffusion-weighted image (C) and apparent diffusion coefficient map (D) showing that the diffusion in the mass is not restricted.

performed to differentiate between sparganosis and echinococcosis four years after surgery. At this time, the antibody titers for *Sparganum* and *Echinococcus* antigen were both below the cutoff values.

He underwent CT scans every 6 mo. During four years of follow-up, the mass in the liver exhibited no change in size or other aspects of appearance.

DISCUSSION

The radiologic characteristics of sparganosis in cerebral, scrotal, mammillary, and musculoskeletal areas have been described in several articles[7-13]. Serpiginous tubular structures have been reported in the breast, scrotal, and musculoskeletal sparganosis[11-13]. One reported scrotal sparganosis exhibited multiple serpiginous tubular echogenic structures surrounded by low echoic rims in an echogenic mass, and these findings were similar to the US findings from our case[11]. According to previous reports, serpiginous echogenic tubular structures and surrounding echogenic masses are indicative of sparganum larvae and granulomatous inflammation, respectively[11-13].

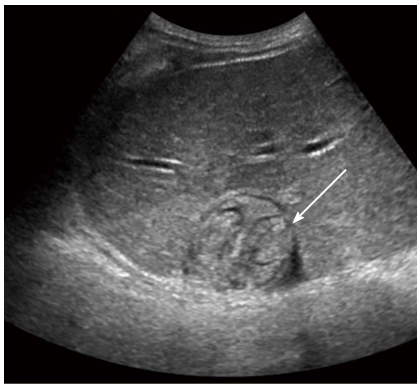

Figure 3 Liver ultrasonography showing a well-defined mixed echoic mass (arrow) in the dome of the liver. Multiple cord-like structures can be seen within the mass.

The two cases of hepatic sparganosis that have been reported thus far presented with large well-defined hepatic abscesses and sparganum larvae coming out of the drains[3,4]. The expelled larvae were flat, long and thread-like (35-40 cm long and 1.5-1.7 mm in width). Sparganum larvae may involve potentially all body tissues but the subcutaneous tissue is the most frequent site[14]. The phenomenon is speculated by the hypothesis that the plerocercoid larvae migrate to the tissue of rather low temperature. Another reason is that subcutaneous sparganosis is more easily detectable than that in deep viscera. In any reason, hepatic sparganosis is extremely rare.

The sensitivity and specificity of the ELISA used in this case are known to be 85.7% and 95.7% for sparganosis and 91.5% and 96% for *Echinococcus*, respectively[15,16]. The high specificity of the ELISA supports the notion that the hepatic mass resulted from sparganum. Overall, based on our imaging findings, initial ELISA test findings and the decreasing trend in the antibody titer for sparganum upon the additional ELISA, we concluded that our case involved a large organizing abscess with dead sparganum larva.

Hydatid cysts caused by *Echinococcus* infection can exhibit internal serpiginous structures due to the detachment of the pericysts and the collapsed membranes inside the cyst, which are collectively called the "snake sign"[6]. However, these collapsed membranes exhibit low signal intensity on all MR imaging sequences, which was not observed on any of the MR images in our case. Typical imaging findings related to hydatid cysts include daughter cysts, floating membranes, internal septa, and thickened walls that represent the pericyst; none of these findings were present in our case.

Calcification on CT images is a common finding of sparganosis, particularly in cerebral sparganosis; up to 75% of all cerebral sparganosis cases have been reported to have calcification[17]. Calcifications represent old lesions in late stages[10]. This finding also supports our diagnosis. The reason that our case had fat foci is unclear but might be related to the process of collagen degeneration in the dead worms.

In conclusion, our case may involve the very rare condition of hepatic sparganosis manifesting as a hepatic mass with calcified serpiginous structures and detailed US, CT, and MR imaging features. The understanding of this case will encourage radiologists and physicians to consider the possibility of hepatic sparganosis when they encounter hepatic masses with bizarrely arranged internal serpiginous structures.

COMMENTS

Case characteristics

A 60-year-old man with rectosigmoid colon cancer having incidentally detected hepatic mass during cancer staging evaluation.

Differential diagnosis

Organizing abscess/hematoma, foreign body granuloma and parasite infestation.

Laboratory diagnosis

Only anti-sparganum antibodies were detected on ELISA test.

Imaging diagnosis

Computed tomography (CT) scan demonstrated a large low-attenuation mass with internal bizarrely arranged cord-like structures, calcifications, and a few focal areas of fat. Liver magnetic resonance (MR) imaging showed serpiginous tubular structures on T2-weighted images. Diffusion in the mass was not restricted on diffusion-weighted MR images. Liver ultrasonography (US) demonstrated a well-demarcated mass with echogenic material and serpiginous echogenic structures.

Experiences and lessons

This case report describes imaging features of rare hepatic sparganosis. Awareness of possibility of hepatic sparganosis can lead to proper diagnostic tests and earlier diagnosis.

Peer-review

The strength of this article is a detailed radiologic description of a presumptive case of hepatic sparganosis, including US, CT, and MR imaging findings.

REFERENCES

1 **Lv S**, Zhang Y, Steinmann P, Zhou XN, Utzinger J. Helminth infections of the central nervous system occurring in Southeast Asia and the Far East. *Adv Parasitol* 2010; **72**: 351-408 [PMID: 20624537 DOI: 10.1016/s0065-308x(10)72012-1]

2 **Cho SY**, Bae JH, Seo BS. Some Aspects Of Human Sparganosis In Korea. *Kisaengchunghak Chapchi* 1975; **13**: 60-77 [PMID: 12913468 DOI: 10.3347/xkjp.1975.13.1.60]

3 **Khurana S**, Appannanavar S, Bhatti HS, Verma S. Sparganosis of liver: a rare entity and review of literature. *BMJ Case Rep* 2012; **2012**: pii: bcr2012006790 [PMID: 23220827 DOI: 10.1136/bcr-2012-006790]

4 **Song CS**, Moon WK, Kang PJ, Lee DW, Yang WS, Huh Y, Moon HK.A case of sparganosis combined with liver abscess. *Korean J Med* 1990; **39**: 686-690

5 **Byun SJ**, Moon KC, Suh KS, Han JK, Chai JY. An imported case of echinococcosis of the liver in a Korean who traveled to western and central Europe. *Korean J Parasitol* 2010; **48**: 161-165 [PMID: 20585534 DOI: 10.3347/kjp.2010.48.2.161]

6 **Marrone G**, Crino' F, Caruso S, Mamone G, Carollo V, Milazzo M, Gruttadauria S, Luca A, Gridelli B. Multidisciplinary imaging of liver hydatidosis. *World J Gastroenterol* 2012; **18**: 1438-1447 [PMID: 22509075 DOI: 10.3748/wjg.v18.i13.1438]

7 **Chang KH**, Cho SY, Chi JG, Kim WS, Han MC, Kim CW, Myung H, Choi KS. Cerebral sparganosis: CT characteristics. *Radiology* 1987; **165**: 505-510 [PMID: 3659374 DOI: 10.1148/radiology.165.2.3659374]

8 **Kradel J**, Drolshagen LF, MacDade A. MR and CT findings in cerebral sparganosis. *J Comput Assist Tomogr* 1993; **17**: 989-990 [PMID: 8227593 DOI: 10.1097/00004728-199311000-00028]

9 **Moon WK**, Chang KH, Cho SY, Han MH, Cha SH, Chi JG, Han MC. Cerebral sparganosis: MR imaging versus CT features. *Radiology* 1993; **188**: 751-757 [PMID: 8351344 DOI: 10.1148/radiology.188.3.8351344]

10 **Song T**, Wang WS, Zhou BR, Mai WW, Li ZZ, Guo HC, Zhou F. CT and MR characteristics of cerebral sparganosis. *AJNR Am J Neuroradiol* 2007; **28**: 1700-1705 [PMID: 17885230 DOI: 10.3174/ajnr.A0659]

11 **Kim YJ**, Lee MW, Jeon HJ, Yi JG, Paick SH, Kim HG, Lim SD, Hwang TS. Sparganosis in the scrotum: sonographic findings. *J Ultrasound Med* 2007; **26**: 129-131 [PMID: 17182719]

12 **Hong SJ**, Kim YM, Seo M, Kim KS. Breast and scrotal sparganosis: sonographic findings and pathologic correlation. *J Ultrasound Med* 2010; **29**: 1627-1633 [PMID: 20966474]

13 **Cho JH**, Lee KB, Yong TS, Kim BS, Park HB, Ryu KN, Park JM, Lee SY, Suh JS. Subcutaneous and musculoskeletal sparganosis: imaging characteristics and pathologic correlation. *Skeletal Radiol* 2000; **29**: 402-408 [PMID: 10963426 DOI: 10.1007/s002560000206]

14 **Liu Q**, Li MW, Wang ZD, Zhao GH, Zhu XQ. Human sparganosis, a neglected food borne zoonosis. *Lancet Infect Dis* 2015; **15**: 1226-1235 [PMID: 26364132 DOI: 10.1016/s1473-3099(15)00133-4]

15 **Kim H**, Kim SI, Cho SY. Serological Diagnosis Of Human Sparganosis By Means Of Micro-ELISA. *Kisaengchunghak Chapchi* 1984; **22**: 222-228 [PMID: 12891016 DOI: 10.3347/kjp.1984.22.2.222]

16 **Jin Y**, Anvarov K, Khajibaev A, Hong S, Hong ST. Serodiagnosis of echinococcosis by ELISA using cystic fluid from Uzbekistan sheep. *Korean J Parasitol* 2013; **51**: 313-317 [PMID: 23864742 DOI: 10.3347/kjp.2013.51.3.313]

17 **Chang KH**, Chi JG, Cho SY, Han MH, Han DH, Han MC. Cerebral sparganosis: analysis of 34 cases with emphasis on CT features. *Neuroradiology* 1992; **34**: 1-8 [PMID: 1553030 DOI: 10.1007/BF00588423]

P- Reviewer: Cerwenka H, Huang CT, Torres US **S- Editor**: Kong JX
L- Editor: A **E- Editor**: Li D

Published by **Baishideng Publishing Group Inc**
8226 Regency Drive, Pleasanton, CA 94588, USA
Telephone: +1-925-223-8242
Fax: +1-925-223-8243
E-mail: bpgoffice@wjgnet.com
Help Desk: http://www.wjgnet.com/esps/helpdesk.aspx
http://www.wjgnet.com